bioRxiv preprint doi: https://doi.org/10.1101/556159; this version posted February 20, 2019. The copyright holder for this preprint (which was not certified by peer review) is the author/funder, who has granted bioRxiv a license to display the preprint in perpetuity. It is made available under aCC-BY 4.0 International license.

PLoS Pathogens

An insect serotonin receptor mediates cellular immune responses and its inhibition by phenylethylamide derivatives from bacterial secondary metabolites

Md Ariful Hasan[1], Hyun-Suk Yeom[2], Jaewook Ryu[2], Helge B. Bode[3], Yonggyun Kim[1,*]

[1] Department of Plant Medicals, College of Life Sciences, Andong National University, Andong 36729, Korea. [2] Center for Eco-Friendly New Materials, Korea Research Institute of Chemicals Technology, Yuseong, Daejeon 34114, Korea. [3] Department of Biosciences, Molecular Biotechnology, and Buchmann Institute for Molecular Life Sciences (BMLS), Goethe-Universität Frankfurt am Main, Germany

* Corresponding author: hosanna@anu.ac.kr

bioRxiv preprint doi: https://doi.org/10.1101/556159; this version posted February 20, 2019. The copyright holder for this preprint (which was not certified by peer review) is the author/funder, who has granted bioRxiv a license to display the preprint in perpetuity. It is made available under aCC-BY 4.0 International license.

Abstract

Serotonin (5-hydroxytryptamine: 5-HT) is a biogenic monoamine that mediates immune responses and modulates nerve signal in insects. *Se-5HTR*, a specific receptor of serotonin, has been identified in the beet armyworm, *Spodoptera exigua*. It is classified into subtype 7 among known 5HTRs. *Se-5HTR* was expressed in all developmental stages of *S. exigua*. It was expressed in all tested tissues of larval stage. Its expression was up-regulated in hemocytes and fat body in response to immune challenge. RNA interference (RNAi) of *Se-5HTR* exhibited significant immunosuppression by preventing cellular immune responses such as phagocytosis and nodulation. Treatment with an inhibitor (SB-269970) specific to 5HTR subtype 7 resulted in significant immunosuppression. Such immunosuppression was also induced by bacterial secondary metabolites derived from *Xenorhabdus* and *Photorhabdus*. To determine specific bacterial metabolites inhibiting Se-5HTR, this study screened 37 bacterial secondary metabolites with respect to cellular immune responses associated with Se-5HTR and selected 10 potent inhibitors. These 10 selected compounds competitively inhibited cellular immune responses against 5-HT and shared phenylethylamide (PEA) chemical skeleton. Subsequently, 46 PEA derivatives were screened and resulting potent chemicals were used to design a compound to be highly inhibitory against Se-5HTR. The designed compound was chemically synthesized. It showed high immunosuppressive activities along with specific and competitive inhibition activity for Se-5HTR. This study reports the first 5HT receptor from *S. exigua* and provides its specific inhibitor designed from bacterial metabolites and their derivatives.

bioRxiv preprint doi: https://doi.org/10.1101/556159; this version posted February 20, 2019. The copyright holder for this preprint (which was not certified by peer review) is the author/funder, who has granted bioRxiv a license to display the preprint in perpetuity. It is made available under aCC-BY 4.0 International license.

41 **Author Summary**

42 Serotonin (5-hydroxytryptamine: 5-HT) plays a crucial role in mediating nerve and immune
43 signals in insects. Interruption of 5-HT signal leads to malfunctioning of various insect
44 physiological processes. Se-5HTR, a 5-HT receptor of beet armyworm, *Spodoptera exigua*, was
45 identified and classified as subtype 7 (5-HT_7) of 5-HT receptors. A specific inhibitor (SB-269970)
46 for 5-HT_7 highly inhibited immune responses such as phagocytosis and nodulation mediated by
47 Se-5HTR. Two entomopathogenic bacteria, *Xenorhabdus* and *Photorhabdus*, could secrete
48 potent inhibitors against immune responses mediated by 5-HTR. Bacterial secondary metabolites
49 were screened against Se-5HTR-mediating immune responses. Most of resulting compounds
50 shared phenylethylamide (PEA) chemical skeleton. Subsequent screening using PEA derivatives
51 supported the importance of this chemical skeleton. Based on their relative inhibitory activities, a
52 compound was designed and synthesized. This novel compound possessed high inhibitory
53 activities against Se-5HTR-mediating immune responses and exhibited competitive inhibition
54 with 5-HT.

55

bioRxiv preprint doi: https://doi.org/10.1101/556159; this version posted February 20, 2019. The copyright holder for this preprint (which was not certified by peer review) is the author/funder, who has granted bioRxiv a license to display the preprint in perpetuity. It is made available under aCC-BY 4.0 International license.

Introduction

Serotonin or 5-hydroxytryptamine (5-HT) is a biogenic monoamine found across most phyla of life [1]. This indolamine compound is biosynthesized from tryptophan by successive catalytic activities of tryptophan hydroxylase and aromatic-L-amino acid decarboxylase [2-4] primarily in nervous systems [5,6]. In human and other vertebrates, serotonin is a well-known neurotransmitter involved in mood, appetite, sleep, anxiety, cognition, and psychosis [7-9]. Outside the nervous system, serotonin plays important roles as growth factor and regulator of hemostasis and blood clotting [10,11]. In plants, serotonin is basically involved in stress signaling [12]. Serotonin plays crucial role in physiological and behavioral processes in insects and other invertebrates [13,14]. In *Drosophila melanogaster*, there is evidence that serotonin is required for courtship and mating [15], circadian rhythm [16,17], sleep [18], locomotion [13,19], aggression [20], insulin signaling and growth [21], and phagocytosis [22]. Serotonin is also involved in olfactory processing [23], feeding behavior [19], heart rate [24], and responses to light [25] in *D. melanogaster* larvae.

Serotonin modulates physiological processes by binding to specific receptors. Seven main subtypes of serotonin receptors have been classified in vertebrates [26]. Except 5-HT_3 receptor, the other six classes (5-HT_1, 5-HT_2, 5-HT_4, 5-HT_5, 5-HT_6, and 5-HT_7 receptors) belong to G protein-coupled receptor family [27]. Among these receptors, 5-HT_1 and 5-HT_5 receptors can inhibit cAMP synthesis by preferentially coupling to a trimeric G protein $G_{i/o}$ [28]. 5-HT_2 receptor uses $G_{q/11}$ to induce breakdown of inositol phosphates, resulting in an increase in cytosolic Ca^{2+} level [28]. Besides, 5-HT_4, 5-HT_6, and 5-HT_7 receptors coupled to G_s can stimulate cAMP production [28]. However, 5-HT_3 receptor is a ligand-gated cation channel that mediates neuronal depolarization [29].

bioRxiv preprint doi: https://doi.org/10.1101/556159; this version posted February 20, 2019. The copyright holder for this preprint (which was not certified by peer review) is the author/funder, who has granted bioRxiv a license to display the preprint in perpetuity. It is made available under aCC-BY 4.0 International license.

Insects have at least three subtypes of 5-HT receptors. Five different 5-HT receptors as orthologous to mammalian 5-HT_{1A}, 5-HT_{1B}, 5-HT_{2A}, 5-HT_{2B}, and 5-HT_7 have been identified in *D. melanogaster* [14]. In addition, partial sequences of two 5-HT_1, two 5-HT_2, and one 5-HT_7 receptors have been identified in the field cricket *Gryllus bimaculatus* [30]. Two 5-HT_1 receptors and two 5-HT_1 splice variants have been described in *Tribolium castaneum* and *Papilio xuthus*, respectively [31,32]. As from *D. melanogaster* and *G. bimaculatus*, two 5-HT_2 receptors have been described from *Apis mellifera* while only one 5-HT_2 receptor has been reported in other insects such as *Periplaneta americana* and *Locusta migratoria* [33,34]. In a lepidopteran species, *Pieris rapae*, four different 5-HT receptors including a novel subtype 8 have been reported [35,36].

5-HT modulates various physiological processes via expression of different receptor types in various tissues. 5-HT receptors are expressed highly in brain and ventral nerve cord of insects [32]. 5-HT_1 receptor in honey bee brain is involved in visual information processing [37]. Expression pattern of 5-HT_7 receptor in honey bee nervous system suggests its possible roles in information processing, learning, and memory [38]. 5-HT receptors might play roles in neuroendocrine secretion and gut motility in cockroaches [29]. In salivary gland of several insects, 5-HT_7 receptor has been reported to be involved in salivary secretion mediated by cAMP level elevation [33,39,40]. Moreover, 5-HT_7 receptor mediates visceral muscle contraction in the gastrointestinal tract of several insects including *A. aegypti* and *T. castaneum* [41,42]. 5-HT not only has neurophysiological roles, but also mediates cellular immune responses in insects by enhancing phagocytosis and nodulation [43]. Two different 5-HT receptors (1B and 2B) are expressed in hemocytes of *P. rapae*, of which 5-HT receptor 1B mediates cellular immune response [22]. In another lepidopteran insect, *Spodoptera exigua*, 5-HT mediates increase of total

bioRxiv preprint doi: https://doi.org/10.1101/556159; this version posted February 20, 2019. The copyright holder for this preprint (which was not certified by peer review) is the author/funder, who has granted bioRxiv a license to display the preprint in perpetuity. It is made available under aCC-BY 4.0 International license.

102 circulatory hemocyte number by stimulating sessile hemocytes and mediating cellular immune
103 responses such as phagocytosis and nodule formation [44,45]. However, 5-HT receptor in *S.*
104 *exigua* has not been reported yet.

105 Two entomopathogenic bacteria, *Xenorhabdus* and *Photorhabdus*, can inhibit insect immune
106 responses to protect themselves and their symbiotic nematodes [46]. To accomplish host
107 immunosuppression, these bacteria can synthesize and secrete secondary metabolites to inhibit
108 immune signals and effectors [47]. Among these bacterial metabolites, tryptamine and
109 phenylethylamide derivatives have been identified with suggested function of interrupting 5-HT
110 signaling [48]. The objective of the present study was to determine bacterial secondary
111 compound(s) that could inhibit 5-HT signaling. To this end, we identified 5-HT receptor that
112 could mediate insect immunity in *S. exigua*. To determine a potent inhibitor of this receptor, we
113 screened bacterial secondary metabolites and their potent derivatives.

114

115 **Results**

116 **Bioinformatics analyses reveal that *S. exigua* contains a 5-HT receptor**

117 From a short read archive database (GenBank accession number: SRR1050532) of *S. exigua*, a
118 highly matched contig (accession number: GARL01017386.1) containing 3,308 bp nucleotide
119 sequence with an open reading frame (ORF) from 996th to 2,690th bp was identified. Prediction
120 of amino acid sequence by BlastP analysis revealed that its ORF sequence shared identities with
121 other insect 5-HT receptors: 99% with *Spodoptera litura* 5HTR (XP_022827337.1), 98% with
122 *Helicoverpa armigera* 5HTR (XP_021195909.1), 95% with *Trichoplusia ni* 5HTR
123 (XP_026729862.1), and 85% with *Manduca sexta* 5HTR (AGL46976.1). This novel 5-HT
124 receptor from *S. exigua* (Se-5HTR) encoded a sequence of 564 amino acids having a predicted

bioRxiv preprint doi: https://doi.org/10.1101/556159; this version posted February 20, 2019. The copyright holder for this preprint (which was not certified by peer review) is the author/funder, who has granted bioRxiv a license to display the preprint in perpetuity. It is made available under aCC-BY 4.0 International license.

molecular weight of about 63.23 kDa. Phylogenetic analysis of its protein sequence indicated that Se-5HTR was clustered with other 5-HT_7 receptors (Fig 1A). Predicted amino acid sequence of Se-5HTR contained a signal peptide of 35 residues and attained GPCR character with seven transmembrane domains. Consensus N-linked glycosylation sites are located in the N-terminus (Asn^{48} and Asn^{53}), the third intracellular loop (Asn^{362}), and C-terminus (Asn^{534}). Several consensus sites for phosphorylation by protein kinase A and/or protein kinase C were predicted throughout the length of the sequence. A disulfide bond between two Cys residues at extracellular matrix ('ECM', S1 Fig) is also predicted.

Se-5HTR sequence attains highly conserved amino acid residues (Fig 1B) found uniquely in the biogenic monoamine receptor family [49-51]. Negatively charged Asp residue in TM3 (Asp^{163}) might interact with positively charged amino group of the ligand. A hydrogen bond between the hydroxyl group of serine residue in TM5 (Ser^{247}) and the hydroxyl group of 5-HT was predicted. In TM6, the consensus sequence unique to aminergic receptors (Phe^{444}-X-X-X-Trp^{448}-X-Pro^{450}-X-Phe^{452}) is conserved. Like other GPCRs, a possible motif (Asn^{485}-Pro^{486}-X-X-Tyr^{489}) that might participate in agonist-mediated sequestration and re-sensitization of Se-5HTR is conserved in TM7. The C-terminus of the receptor contains two potential post-translational palmitoylation cysteine residues (Cys^{508} and $Cys-^{532}$) and PDZ (post synaptic density protein, *Drosophila* disc large tumor suppressor, and zonula occludens-1 protein)-domain binding motif (Glu^{561}-Ser^{562}-Phe^{563}-Leu^{564}).

Se-5HTR is expressed in all developmental stages and larval tissues

Expression of *Se-5HTR* in different developmental stages of *S. exigua* was assessed by RT-PCR. Results showed its expression from egg to adult stages (Fig 2A). RT-qPCR revealed variation in

bioRxiv preprint doi: https://doi.org/10.1101/556159; this version posted February 20, 2019. The copyright holder for this preprint (which was not certified by peer review) is the author/funder, who has granted bioRxiv a license to display the preprint in perpetuity. It is made available under aCC-BY 4.0 International license.

its expression among developmental stages, with L5 larvae and adults showing the highest expression levels. In L5 larvae, all tissues analyzed by RT-PCR showed its expression (Fig 2B). RT-qPCR revealed that the midgut exhibited the highest expression level of *Se-5HTR*. Hemocytes and brain also showed relatively high levels of its expression. Basal expression levels of *Se-5HTR* were highly up-regulated in response to immune challenge (Fig 2C). *Se-5HTR* expression was increased ~125-fold after challenge with fungus, *Beauveria bassiana* compared to control (unchallenged). It was increased 60~90-fold after bacterial challenge compared to naïve larvae.

Specific inhibitors against 5-HTR suppress hemocyte behaviors of *S. exigua*

A commercial inhibitor (SB-269970) specific to 5-HT_7 was used to assess its effect on hemocyte behaviors of *S. exigua* (Fig 3). Total hemocyte count (THC) of L5 larvae was ~1.2×10^7 cells/mL (Fig 3A). THC was significantly ($P < 0.05$) increased in response to 5-HT or bacterial challenge. SB-269970 prevented the increase of THC in response to bacterial challenge. Its IC_{50} value was estimated to be 1.925 μM. These results suggest that Se-5HTR can mediate hemocyte mobilization in response to 5-HT upon bacterial challenge.

To determine the modulation effect of Se-5HTR on hemocyte-spreading behavior, competitive inhibition between SB-269970 and 5-HT against Se-5HTR was assessed (Fig 3B). Hemocytes were spread on slide glass with growth of F-actin. However, SB-269970 significantly ($P < 0.05$) suppressed such hemocyte-spreading behavior. The inhibitory effect of the inhibitor was rescued by addition of 5-HT. A relatively low dose (SB-269970: 5-HT = 10:1) of 5-HT did not rescue the inhibitory effect. However, a relatively high dose (1:10) of 5-HT significantly ($P < 0.05$) rescued such inhibitory effect, indicating a specific competition between inhibitor and

bioRxiv preprint doi: https://doi.org/10.1101/556159; this version posted February 20, 2019. The copyright holder for this preprint (which was not certified by peer review) is the author/funder, who has granted bioRxiv a license to display the preprint in perpetuity. It is made available under aCC-BY 4.0 International license.

171 ligand against Se-5HTR.

172

173 **RNA interference (RNAi) of Se-5HTR**

174 To address the immunomodulatory effect of Se-5HTR on hemocytes, its gene expression was
175 knocked-down by RNAi (Fig 4). RNAi was performed using dsRNA specific to *Se-5HTR*.
176 dsRNA-injected larvae exhibited significant ($P < 0.05$) reduction of *Se-5HTR* expression. RT-
177 qPCR analysis showed that about 90% of *Se-5HTR* mRNA was suppressed by dsRNA treatment
178 at 24 h PI (Fig 4A). At 24 h PI of dsRNA, *Se-5HTR* expression was analyzed in four different
179 tissue samples. Compared to control tissues, dsRNA-treated larvae exhibited significant ($P <$
180 0.05) reduction of *Se-5HTR* expression in all tissues including hemocytes.

181

182 **RNAi of Se-5HTR suppresses hemocyte behaviors of *S. exigua***

183 The effect of RNAi specific to Se-5HTR on hemocyte mobilization in response to bacterial
184 challenge was analyzed (Fig 4B). Upon bacterial challenge, THC increased by more than two
185 folds. However, RNAi treatment significantly ($P < 0.05$) suppressed such increase of THC. The
186 RNAi treatment also significantly ($P < 0.05$) influenced hemocyte-spreading behavior (Fig 4C).
187 On glass slide, hemocytes exhibited spreading behavior in 40 min by cytoskeletal rearrangement
188 through F-actin growth (see phalloidin staining). However, hemocytes collected from larvae
189 treated with RNAi specific to Se-5HTR lost such behavior.

190

191 **Modulation of cellular immune responses by Se-5HTR**

192 The influence of Se-5HTR on modulating hemocyte-spreading behavior suggested that it might
193 mediate cellular immune responses against bacterial infection. Phagocytosis against FITC-

bioRxiv preprint doi: https://doi.org/10.1101/556159; this version posted February 20, 2019. The copyright holder for this preprint (which was not certified by peer review) is the author/funder, who has granted bioRxiv a license to display the preprint in perpetuity. It is made available under aCC-BY 4.0 International license.

194 labeled *Escherichia coli* was observed in hemocytes from control larvae. Labeled bacteria were
195 observed within hemocytes of control larvae (Fig 5A). However, hemocytes of larvae treated
196 with dsRNA specific to Se-5HTR significantly ($P < 0.05$) lost such phagocytosis, similar to that
197 found for hemocytes of larvae treated with SB-269970. Phagocytosis was decreased around 57%
198 or 78% after treatment with dsRNA or inhibitor, respectively. In response to bacterial challenge,
199 *S. exigua* formed ~78 hemocytic nodules per larva (Fig 5B). However, RNAi specific to Se-
200 5HTR or inhibitor treatment significantly ($P < 0.05$) reduced such cellular immune response.
201
202 **Influence of bacterial secondary metabolites on immune responses mediated by Se-5HTR**
203 RNAi or specific inhibitor assays indicated that 5-HTR could mediate both cellular immune
204 responses of phagocytosis and nodule formation in response to bacterial challenge. Bacterial
205 metabolites of two entomopathogens, *Xenorhabdus nematophila* (Xn) and *Photorhabdus*
206 *temperata temperata* (Ptt), were extracted from their culture broth using different organic
207 solvents and their inhibitory activities against cellular immune responses were then assessed (Fig
208 6). Organic solvent extracts of Xn- or Ptt-cultured broth exhibited significant ($P < 0.05$)
209 inhibitory activities against phagocytosis (Fig 6A) and nodulation (Fig 6B), although there were
210 variations in their inhibitory activities among extracts.
211 To identify bacterial secondary compounds that could inhibit Se-5HTR, 37 compounds (HB4
212 – HB602) derived from *Xenorhabdus* and *Photorhabdus* [47] were screened for their inhibitory
213 activities against hemocyte nodule formation and phagocytosis (Fig 7). More than three 75% (28
214 out of 37 compounds) of these test compounds exhibited significant ($P < 0.05$) inhibition against
215 phagocytosis (Fig 7A). In nodulation assay, all test compounds exhibited significant ($P < 0.05$)
216 inhibition (Fig 7B). Since Se-5HTR could mediate both cellular immune responses, bacterial

bioRxiv preprint doi: https://doi.org/10.1101/556159; this version posted February 20, 2019. The copyright holder for this preprint (which was not certified by peer review) is the author/funder, who has granted bioRxiv a license to display the preprint in perpetuity. It is made available under aCC-BY 4.0 International license.

compounds that highly inhibited both phagocytosis (□ 60%) and nodulation (□ 30 nodules per larva) were selected. As a result, 10 potent chemicals (HB 4, HB 5, H23, HB 30, HB44, HB 45, HB 50, HB 223, HB 302, and HB 531) belonging to six chemical categories [phenylethylamide (PEA), tryptamide, xenortide, xenocycloin, nematophin, and GameXPeptide] were found (S2 Fig). All these compounds exhibited median inhibitory concentration (IC_{50}) of 58~253 μM against cellular immune response of hemocytic nodulation.

To support the specific inhibitory activity of these selected compounds against Se-5HTR, competitive assay was performed between test compounds and 5-HT (Fig 8). With a constant concentration of 5-HT, phagocytotic behavior of *S. exigua* hemocytes gradually decreased with increasing amount of test compound (Fig 8A). On the other hand, increase of 5-HT amount gradually decreased the phagocytotic behavior using a constant amount of test compound (Fig 8B).

Influence of PEA derivatives on phagocytosis mediated by Se-5HTR

These 10 selected compounds shared phenyl (or aromatic) ethylamide backbone except xenocycloin (S2 Fig). Based on PEA backbone, 45 derivatives were selected from a chemical bank and their inhibitory activities against the phagocytotic behavior of *S. exigua* hemocytes were tested (Fig 9A). More than 66% (30 out of 45 compounds) of PEA derivatives exhibited significant ($P < 0.05$) inhibition against phagocytosis. Three PEA derivatives (Ph15, Ph17, Ph33) had inhibitory activities similar to a bacterial metabolite (HB 44), with IC_{50} at 1.8 ~ 5.6 μM against phagocytosis (Fig 9B). These three PEA derivatives competitively inhibited the phagocytosis mediated by Se-5HTR (Fig 9C).

bioRxiv preprint doi: https://doi.org/10.1101/556159; this version posted February 20, 2019. The copyright holder for this preprint (which was not certified by peer review) is the author/funder, who has granted bioRxiv a license to display the preprint in perpetuity. It is made available under aCC-BY 4.0 International license.

Synthesis of a potent inhibitor and inhibitory efficacy against Se-5HTR

Potent compounds from 45 PEA derivatives were analyzed for their structures and activities against phagocytosis mediated by Se-5HTR (S3 Fig). They shared the PEA backbone. However, they had different side chains at 'X' and 'Y' (Fig S6A). When different X substituents were compared for their inhibitory activities, methoxy was the most potent moiety (Fig S6B). When different Y substituents were compared for their inhibitory activities with respect to identical X groups, hexahydropyrrolo[1,2-a]pyrazine-1,4-dione was the most potent moiety (Fig S6C). This analysis allowed us to design a hypothetical compound containing methoxy in X and hexahydropyrrolo[1,2-a]pyrazine-1,4-dione at Y based on PEA backbone (Fig. S6D).

The designed compound ('PhX') was chemically synthesized and in its inhibitory activity against phagocytosis was assessed compared with a specific 5-HT_7 inhibitor, SB269970, as a reference (Fig 10). PhX was highly potent. It competitively inhibited cellular immune response with 5-HT. Its inhibitory activity was more potent (t = 14.9; df = 32; P □ 0.0001) than SB269970.

Discussion

5-HT plays a crucial role in mediating cellular immune responses of *S. exigua* by stimulating actin rearrangement [45]. Furthermore, it performs a functional cross-talk with eicosanoid signaling via a small G protein Rac1 [52]. However, its signaling pathway leading to immune responses remains unclear due to the lack of its receptor information in *S. exigua*. This study identified a 5-HT receptor and showed its physiological function in mediating immune responses.

Se-5HTR attains seven transmembrane domains and shares common molecular characters with other 5-HT receptors. Like other GPCRs, Se-5HTR contains the canonical seven transmembrane domains along with consensus glycosylation in the N-terminus (Asn^{48} and Asn^{53})

bioRxiv preprint doi: https://doi.org/10.1101/556159; this version posted February 20, 2019. The copyright holder for this preprint (which was not certified by peer review) is the author/funder, who has granted bioRxiv a license to display the preprint in perpetuity. It is made available under aCC-BY 4.0 International license.

263 [53]. Additionally, its sequence contains a consensus aspartic acid residue in TM3 (Asp^{163}) and a
264 serine residue in TM5 (Ser^{247}) to interact with functional groups of biogenic monoamines [54].
265 At the intracellular border of TM3, the highly conserved Asp^{180}-Arg^{181}-Tyr^{182} motif is evident for
266 a strong ionic interaction with Glu^{430} residue adjacent to the intracellular end of TM6 that plays a
267 crucial role in GPCR signal transduction [55]. The sequence contains consensus Phe^{444}-X-X-X-
268 Trp^{448}-X-Pro^{450}-X-Phe^{452} motif in TM6 which is unique to biogenic monoamine GPCRs [38].
269 Additionally, Se-HTR contains two potential post-translational palmitoylation cysteine residues
270 (Cys^{508} and Cys^{532}) [56] at the final intracellular region with a PDZ-domain binding motif
271 (Glu^{561}-Ser^{562}-Phe^{563}-Leu^{564}) at the C-terminus [57].

272 *Se-5HTR* is expressed in all developmental stages. It is expressed in immune-associated
273 tissues (hemocytes and fat body), digestive (gut) tissues, and nervous (brain) tissues at larval
274 stage. Three 5-HT receptors of *P. rapae* larvae are all expressed, although their expression levels
275 in tissues are different. Subtypes 1A and 1B receptor are highly expressed in nervous tissues
276 while subtype 7 receptor is mainly expressed in digestive tissue [36]. *Se-5HTR* was also highly
277 expressed in the gut like 5-HT_7 of *P. rapae*. Furthermore, our phylogenetic analysis of 5-HT
278 receptors showed that these two insect 5-HT_7s were closely related and clustered. Expression
279 levels of *Se-5HTR* in hemocytes were similar to those in the brain. This suggests that Se-5HTR is
280 associated with immune function as well as neurophysiological function. Indeed, bacterial or
281 fungal infection up-regulated the expression of *Se-5HTR*. The increase of *Se-5HTR* expression
282 might be explained by the up-regulation of *de novo* biosynthesis of its ligand, 5-HT, via increase
283 in expression of biosynthetic genes as seen in hemocytes of *P. rapae* larvae after immune
284 challenge [22].

bioRxiv preprint doi: https://doi.org/10.1101/556159; this version posted February 20, 2019. The copyright holder for this preprint (which was not certified by peer review) is the author/funder, who has granted bioRxiv a license to display the preprint in perpetuity. It is made available under aCC-BY 4.0 International license.

285 The presence of 5-HT_7 receptor in hemocytes of *S. exigua* and its physiological function
286 associated with immune responses were supported by its sensitivity to specific 5-HTR inhibitors.
287 In response to 5-HT or bacterial challenge, *S. exigua* larvae exhibited significant increase of
288 THC. This up-regulation of THC was explained by mobilization of sessile hemocytes to
289 circulatory form by cytoskeletal rearrangement via a small G protein, Rac1 [45,52]. This
290 suggests that Se-5HTR can activate Rac1 to stimulate the hemocyte behavior. In vertebrates,
291 activation of 5-HT_7 receptor increases cAMP level via a trimeric G protein G_s and small G
292 proteins of Rho family including Cdc42, RhoA, and Rac1 via another trimeric G protein G_{12} [58].
293 This suggests that immune challenge can induce biosynthesis and release of 5-HT which then
294 binds to Se-5HTR on hemocytes and activates Rac1 to stimulate hemocyte behaviors. In addition,
295 the cAMP pathway triggered by Se-5HTR might activate Akt and ERK1/2 as seen in mammalian
296 cancer cells [59] to facilitate actin rearrangement to form cellular shape change of hemocytes.
297 These findings suggest that Se-5HTR plays a crucial role in hemocyte migration and cell shape
298 change during cellular immune responses. Indeed, RNAi of *Se-5HTR* expression resulted in
299 significant immunosuppression by exhibiting reduction in phagocytosis and nodulation.

300 Bacterial metabolites derived from two entomopathogens, *Xenorhabdus* and *Photorhabdus*,
301 inhibited cellular immune responses mediated by Se-5HTR. Especially, six chemical groups
302 (phenylethylamide, tryptamide, xenortide, xenocycloin, nematophin, and GameXPeptide) highly
303 inhibited both phagocytosis and nodulation, suggesting that they can inhibit Se-5HTR. This was
304 supported by their competitive inhibition with the ligand, 5-HT. Bacterial secondary metabolites
305 may be synthesized and released in the bacterium-nematode complex in order to defend immune
306 attack from target insect to compete with other microbes occurring in the insect cadaver and
307 facilitate host nematode development or bacterial quorum sensing [47]. It has been reported

bioRxiv preprint doi: https://doi.org/10.1101/556159; this version posted February 20, 2019. The copyright holder for this preprint (which was not certified by peer review) is the author/funder, who has granted bioRxiv a license to display the preprint in perpetuity. It is made available under aCC-BY 4.0 International license.

phenylethylamides and tryptamides identified from *Xenorhabdus* can act as quorum quenching activators by competitive binding to N-acylated homoserine lactone (AHL) receptor because AHL accumulation drives gene expression of bioluminescence, virulence factor, and biofilm formation in bacteria [60,61]. Xenortides are linear peptides consisting of 2-8 amino acids synthesized from both *Xenorhabdus* and *Photorhabdus* [62]. They are synthesized in insect hosts during infection with putative role in inhibiting prophenoloxidase activation to suppress insect immunity [63]. Xenocycloins produced by *X. bovienii* are cytotoxic to hemocytes of *Galleria melonella* [64]. Nematophin is synthesized by condensation of α-keto acid and tryptamine in *X. nematophila*. It possesses a specific antibacterial activity against *Staphylococcus aureus* [65]. GameXPeptides are cyclic pentapeptides widely synthesized in both *Xenorhabdus* and *Photorhabdus*. However, their biological functions remain unclear [66]. This current study showed that these six compound classes could inhibit cellular immune responses by competitive inhibition with 5-HT against Se-5HTR.

A novel phenylethylamide compound, PhX, was found to be highly inhibitory against Se-5HTR. Derivatives of phenylethylamide compound (HB 4) exhibited different inhibitory activities against cellular immune responses mediated by Se-5HTR. Especially, PhX containing methoxy and hexahydropyrrolo[1,2-a]pyrazine-1,4-dione exhibited the highest inhibitory activity. 5-HT receptors have been used for screening for potent insecticides with growth-inhibiting or larvicidal activities against *Pseudaletia separata* [67]. Thus, PhX can be a candidate for this application unless it shows mammalian or non-target species toxicity [68].

Materials and methods

Insect rearing and microbial culture

bioRxiv preprint doi: https://doi.org/10.1101/556159; this version posted February 20, 2019. The copyright holder for this preprint (which was not certified by peer review) is the author/funder, who has granted bioRxiv a license to display the preprint in perpetuity. It is made available under aCC-BY 4.0 International license.

A laboratory strain of *S. exigua* was originated from Welsh onion field (Andong, Korea) and maintained for ~20 years. Larvae of this laboratory strain were reared on an artificial diet [69] at temperature of 25 ± 1°C and relative humidity of 60 ± 10% with a photoperiod of 16:8 h (L:D). Under these conditions, larvae had five instars ('L1-L5'). Adults were reared with 10% sucrose solution. For immune challenge, *Escherichia coli* Top10 (Invitrogen, Carlsbad, CA, USA) was cultured in Luria-Bertani (LB) medium (BD Korea, Seoul, Korea) in a shaking incubator (200 rpm) at 37°C overnight (16 h).

Chemicals

Serotonin hydrochloride was purchased from Sigma-Aldrich Korea (Seoul, Korea). It was dissolved in distilled water. SB-269970 (a specific inhibitor to 5-HT receptor subtype 7, 5-HT_7) was purchased from Cayman Chemical Company (Korea). It was dissolved in desired concentrations with dimethyl sulfoxide (DMSO). Fluorescein isothiocyanate (FITC) [2-(6-hydroxy-3-oxo-3h-xanthen-9-yl)-5-isothiocyanatobenzoic acid] was purchased from Sigma-Aldrich Korea. It was dissolved in DMSO to make a solution at 10 mg/mL. Anticoagulant buffer (ACB) was prepared using 98 mM NaOH, 186 mM NaCl, 17 mM Na_2EDTA, and 41 mM citric acid at pH 4.5. Phosphate-buffered saline (PBS) was prepared at pH 7.4 with 50 mM sodium phosphate and 0.7% NaCl. Tris-buffered saline (TBS) was prepared using 150 mM NaCl, 50 mM Tris-HCl at pH 7.6. Hank's balanced salt solution (HBSS) was prepared with the following compositions: 8 g NaCl, 400 mg KCl, 40 mg Na_2HPO_4, 60 mg KH_2PO_4, 1 g glucose, 140 mg $CaCl_2$, 120 mg $MgSO_4$, and 350 mg $NaHCO_3$ in 1,000 mL distilled H_2O.

Bioinformatics to search for 5-HT receptor and sequence analysis

bioRxiv preprint doi: https://doi.org/10.1101/556159; this version posted February 20, 2019. The copyright holder for this preprint (which was not certified by peer review) is the author/funder, who has granted bioRxiv a license to display the preprint in perpetuity. It is made available under aCC-BY 4.0 International license.

354 *S. exigua* 5-HT receptor (Se-5HTR) sequence was obtained from GenBank by manual annotation.
355 Briefly, a dopamine receptor sequence (AKR18180.1) of *Chilo suppressalis* was used to screen a
356 transcriptome (SRR1050532) of *S. exigua*. A blast contig (GARL01017386.1) was analyzed for
357 open reading frame (ORF) and the predicted amino acid sequence was used for analysis using
358 BlastP program against GenBank (www.ncbi.nlm.nih.gov). After confirming its high homologies
359 (E value < 10^{-20}) with other known insect 5HTRs, the resulting ORF sequence (= Se-5HTR) was
360 deposited at NCBI-GenBank (accession number: MH025798). Sequence alignment was
361 established using Clustal Omega tool (https://www.ebi.ac.uk/Tools/msa/clustalo/) provided by
362 European Bioinformatics Institution. Phylogenetic tree was generated with Neighbor-joining
363 method using Mega6 and ClustalW programs. Bootstrapping values were obtained with 1,000
364 repetitions to support branch and clustering. Protein domain was predicted using InterPro tool
365 (https://www.ebi.ac.uk/interpro/), pfam (http://pfam.xfam.org), and Prosite
366 (http://prosite.expasy.org/).
367
368 **RNA extraction and cDNA preparation**
369 Using Trizol reagent (Invitrogen), total RNAs were extracted from all developmental stages as
370 well as larval tissues (hemocyte, midgut, fat body, and brain) of *S. exigua* according to the
371 instruction of the manufacturer. Numbers of individuals used for RNA extraction for each
372 individual developmental stage were as follows: ~500 eggs, ~20 larvae for L1-L2, ~10 larvae for
373 L3, ~5 larvae for L4, one larva for L5, one pupa, and one adult. L5 larvae were used for RNA
374 extraction from different tissue samples. After extraction, total RNAs were resuspended in
375 nuclease-free water and cDNAs were synthesized from ~1 μg of RNAs using Maxime RT
376 Premix (Intron Biotechnology, Seoul, Korea) according to the manufacturer's instruction.

bioRxiv preprint doi: https://doi.org/10.1101/556159; this version posted February 20, 2019. The copyright holder for this preprint (which was not certified by peer review) is the author/funder, who has granted bioRxiv a license to display the preprint in perpetuity. It is made available under aCC-BY 4.0 International license.

377

378 **Expression pattern of Se-5HTR by RT-qPCR**

379 A fragment of *Se-5HTR* was amplified with gene-specific primers (5□- CTT TAC CTT CGT
380 GTC TTC TC-3□ and 5□- GGT GTC AGT CTT CTC ATT AC -3□). PCR was performed with
381 35 cycles of denaturation (94°C, 1 min), annealing (49°C, 1 min), and extension (72°C, 1 min).
382 PCR products were subjected to agarose gel electrophoresis to visually confirm their
383 amplifications. With the same gene-specific primers used in RT-PCR, RT-qPCR was performed
384 in a qPCR machine (CFX Connect^{TM} Real-Time PCR Detection System, Bio-Rad, Hercules, CA,
385 USA) using SYBR Green Realtime PCR Master Mix (Toyobo, Osaka, Japan) under a guideline
386 of Bustin et al. [70]. The amplification used 40 cycles of 15 s at 95°C, 30 s at 60°C, and 45 s at
387 72°C. After PCR reactions, melting curves from 60 to 95°C were obtained to confirm unique
388 PCR products. A ribosomal protein, RL32, gene was used as a control with primers of 5□-ATG
389 CCC AAC ATT GGT TAC GG-3□ and 5□-TTC GTT CTC CTG GCT GCG GA-3□. Each
390 treatment was independently triplicated. Relative quantitative analysis method ($2^{-\Delta\Delta CT}$) was used
391 to estimate mRNA expression levels of *Se-5HTR*.

392

393 **RNA interference (RNAi)**

394 Gene fragment of *Se-5HTR* was amplified from template DNA using gene-specific primers (5'-
395 CTT TAC CTT CGT GTC TTC TC-3' and 5'-GGT GTC AGT CTT CTC AT-3') possessing T7
396 RNA polymerase promoter sequence (5'-TAA TAC GAC TCA CTA TAG GGA GA-3') at 5'
397 ends. PCR was performed with 5 cycles of denaturation (94°C, 1 min), annealing (49°C, 1 min),
398 and extension (72°C, 1 min) followed by 30 cycles of denaturation (94°C, 1 min), annealing
399 (60°C, 1 min), and extension (72°C, 1 min) to synthesize DNA template for dsRNA synthesis.

bioRxiv preprint doi: https://doi.org/10.1101/556159; this version posted February 20, 2019. The copyright holder for this preprint (which was not certified by peer review) is the author/funder, who has granted bioRxiv a license to display the preprint in perpetuity. It is made available under aCC-BY 4.0 International license.

Double-stranded RNA (dsRNA) against *Se-5HTR* ('dsSe-5HTR') was synthesized using Megascript RNAi kit (Ambion, Austin, TX, USA) following the manufacturer's instruction. The resulting dsRNA was blended with Metafectene PRO (Biontex, Plannegg, Germany) at 1:1 (v:v) ratio and incubated at 25°C for 30 min for liposome formation. Two microliters of the prepared mixture containing ~900 ng of dsRNA was injected twice into *S. exigua* larval hemocoel using a microsyringe (Hamilton, Reno, NV, USA) equipped with a 26-gauge needle. The first injection was at late L4 stage. It was repeated 12 h afterwards. RNAi efficacy at 0, 24, and 48 h post-injection (PI) in reducing *Se-5HTR* expression was determined by RT-qPCR. At 24 h PI, treated larvae were used for immune challenge experiments. Each treatment was replicated thrice using 10 larvae for each replication.

Total hemocyte count (THC)

Hemolymph was collected by cutting larval proleg and mixed with ACB (1:10, v/v). Hemocytes were counted using a Neubauer hemocytometer (Superior Marienfeld, Lauda-Königshofen, Germany) under a phase contrast microscope (BX41, Olympus, Tokyo, Japan) at 100× magnification. Heat-killed (90°C, 30 min) *Escherichia coli* (5×10^5 cells/larva) and a test chemical (5-HT or SB-269970) were co-injected into hemocoel through abdominal proleg of L5 larvae in a volume of 5 µL using a 10 µL micro-syringe (Hamilton) after surface-sterilization with 70% ethanol. After 4 h of incubation at 25 ± 2°C, hemolymph of the insect was collected and assessed for THC.

Hemocyte-spreading analysis

After hemolymph (~150 µL) was collected from five L5 larvae by cutting prolegs, it was mixed

bioRxiv preprint doi: https://doi.org/10.1101/556159; this version posted February 20, 2019. The copyright holder for this preprint (which was not certified by peer review) is the author/funder, who has granted bioRxiv a license to display the preprint in perpetuity. It is made available under aCC-BY 4.0 International license.

423 with three times volume of ice-cold ACB and incubated on ice for 30 min. ACB-treated
424 hemolymph was then centrifuged at 800 × *g* for 5 min at 4°C. The resulting pellet was re-
425 suspended in 500 µL of filter-sterilized TC-100 insect cell culture medium (Welgene, Daegu,
426 Korea). On a glass coverslip placed in a moist chamber, 10 µL of hemocyte suspension was
427 applied and placed in a dark condition. Hemocytes were then fixed with 4% paraformaldehyde
428 (filter-sterilized) at 25°C for 10 min and then washed thrice with filter-sterilized PBS. Cells were
429 then permeabilized with 0.2% Triton-X dissolved in PBS at 25°C for 2 min and washed with
430 PBS. After that, hemocytes were blocked using 10% bovine serum albumin (BSA) dissolved in
431 PBS at 25°C for 10 min and washed again with PBS. Cells were then incubated with FITC-
432 tagged phalloidin in PBS for 60 min and washed thrice with PBS. Hemocytes nuclei were then
433 stained by incubating with 4′,6-diamidino-2-phenylindole (DAPI, 1 µg/mL) (Thermo Fisher
434 Scientific, Rockford, IL, USA) dissolved in PBS and washed thrice with PBS. Hemocytes were
435 then observed under a fluorescence microscope (DM2500, Leica, Wetzlar, Germany) at 400×
436 magnification. Hemocyte-spreading was dictated by appendages of F-actin outward the
437 hemocyte cell boundary.

438 To assess effect of *Se-5HTR* RNAi on hemocyte-spreading, hemocytes were collected at 24 h
439 after injecting dsSe-5HTR (~900 ng/larva). In separate experiments, 5-HT and 5-HTR inhibitor
440 SB-269970 were co-injected into dsRNA-treated larvae at ratios of 1:10 and 10:1 to check their
441 influence on hemocyte-spreading. At 6 h after co-injection, hemolymph was collected from the
442 treated larva and hemocyte-spreading was observed using the above-mentioned method.

443

444 **Nodulation assay**

445 Overnight culture of *E. coli* Top10 bacterial cells was washed with PBS and centrifuged at 1,120

bioRxiv preprint doi: https://doi.org/10.1101/556159; this version posted February 20, 2019. The copyright holder for this preprint (which was not certified by peer review) is the author/funder, who has granted bioRxiv a license to display the preprint in perpetuity. It is made available under aCC-BY 4.0 International license.

× *g* for 10 min. L5 larvae were used to assess hemocyte nodule formation by immune-challenge with bacterial injection (~1.8 × 10^5 cells/larva) through the abdominal proleg into larval hemocoel using a microsyringe as previously described. To assess the effect of *Se-5HTR* RNAi on nodule formation, bacterial challenge was performed at 24 h after injecting dsSe-5HTR (~900 ng/larva). To check the influence of chemicals on nodule formation, 2 µg of ketanserin and/or 10 µg of 5-HT was co-injected along with the bacterial suspension. In separate experiment, 1 µg of the bacterial secondary metabolite was co-injected with the bacterial suspension to assess immune suppression activity of the test compound. After an incubation period of 8 h at 25°C, treated insects were dissected under a stereo microscope (SZX9, Olympus, Japan) to count melanized nodule numbers. Each treatment was triplicated independently using five insects for each replication.

Phagocytosis assay

Preparation of FITC-labeled bacterial cells followed the method described by Harlow and Lane (1998). Briefly, *E. coli* Top10 cells were cultured in 50 mL of Luria-Bertani broth (37°C, 16 h). These bacterial cells were then harvested by centrifuging 1 mL of the cultured broth at 1,120 × *g* for 10 min at 4°C. Bacterial cells (10^5 cells/mL) were washed twice with TBS and re-suspended in 1 mL of 0.1 M sodium bicarbonate buffer (pH 9.0). In the suspension, 1 µL of 10 mg/mL FITC solution was added and immediately mixed. The mixture was then incubated under darkness with end-over-end rotation at 25°C for 30 min. After the incubation, FITC-tagged bacteria were harvested by centrifugation at 22,000 × *g* for 20 min at 4°C. These bacterial cells were washed thrice with HBSS to remove unbound dye and re-suspended in TBS.

To assess *in vivo* phagocytosis activity, 5 µL of FITC-tagged *E. coli* suspension was injected

bioRxiv preprint doi: https://doi.org/10.1101/556159; this version posted February 20, 2019. The copyright holder for this preprint (which was not certified by peer review) is the author/funder, who has granted bioRxiv a license to display the preprint in perpetuity. It is made available under aCC-BY 4.0 International license.

into the hemocoel of L5 larva through the proleg. To assess the effect of *Se-5HTR* RNAi on phagocytosis activity, bacteria were injected at 24 h after injecting dsSe-5HTR (~900 ng/larva). To check the influence of a specific 5-HT_7 receptor inhibitor on phagocytosis, 2 µg of SB-269970 was co-injected with the tagged bacterial suspension. To determine the effect of secondary metabolite on phagocytosis, 1 µg of bacterial secondary metabolite was co-injected with tagged bacterial suspension. After 15 min of incubation, treated larvae were surface-sterilized using 70% ethanol. With a pair of scissors, the proleg was cut to collect hemolymph sample (~50 µL) in 150 µL of cold ACB with gentle shaking of the tube to mix hemolymph and ACB thoroughly. Hemocyte monolayers were made using 50 µL of hemocyte suspension (~5 × 10^3 cells) and left in a moist chamber for 15 min for hemocytes to settle and attach to the glass surface. After the incubation period, monolayers were washed with TBS to remove plasma. These monolayers were overlaid with 1% trypan blue dye solution to quench non-phagocytosed bacterial cells. After 10 min, monolayers were washed again with TBS and then fixed with 1.5% glutaraldehyde solution to observe under a fluorescence microscope at 400× magnification. Hemocytes undergoing phagocytosis were counted from a total of 100 hemocytes observed from different areas of each slide. Each observation was triplicated with three different slides.

Preparation of organic extracts from bacterial culture broth

X. nematophila K1 (Xn) and *P. temperate temperata* ANU101 (Ptt) bacteria were cultured in TSB at 28°C for 48 h. Culture broths were centrifuged at 12,500 × *g* for 30 min and supernatants were used for subsequent fractionation. To obtain ethyl acetate extract, the same volume (1 L) of ethyl acetate was mixed with the supernatant and separated into organic and aqueous fractions. Ethyl acetate extract ('EAX') was dried using a rotary evaporator (Sunil Eyela, Seongnam,

bioRxiv preprint doi: https://doi.org/10.1101/556159; this version posted February 20, 2019. The copyright holder for this preprint (which was not certified by peer review) is the author/funder, who has granted bioRxiv a license to display the preprint in perpetuity. It is made available under aCC-BY 4.0 International license.

492 Korea) at 40°C. The resulting extract (0.2 mg) was obtained from 1 L cultured broth and
493 resuspended with 5 mL of methanol. The aqueous phase was then combined with 1 L of butanol.
494 Butanol extract ('BX') was also dried using the rotary evaporator at 40°C and the resulting
495 extract (0.2 mg) was resuspended with 5 mL of methanol.
496
497 **Secondary bacterial metabolites – biological activity against immune responses**
498 Secondary metabolites (37 samples, S4 Fig) derived from *Xenorhabdus* and *Photorhabdus*
499 cultures were from the Bode lab compound collection named 'HB' compounds. Their biological
500 activities for suppressing *S. exigua* immunity were then determined. Individual chemicals were
501 dissolved in DMSO, diluted into desired concentrations with DMSO, and stored at -20°C.
502 For hemocyte nodulation inhibition assay, overnight culture of *E. coli* bacterial cells was
503 washed with PBS. Test compound (1 µg/larva) was injected into larval hemocoel along with the
504 bacterial suspension (~1.8×10^5 cfu/larva) using a microsyringe as previously described. Insects
505 were then incubated at 25°C for 8 h. After the incubation period, insects were dissected and
506 nodule numbers were counted as described above. Each treatment was triplicated independently
507 using five insects for each replication. For phagocytosis inhibition assay, 5 µL of FITC-tagged *E.*
508 *coli* suspension along with 1 µg of test compound was injected into L5 larval hemocoel. After 15
509 min of incubation period, hemocytes undergoing phagocytosis were counted as previously
510 described.
511
512 **Secondary bacterial metabolites – competitive assay with 5-HT**
513 To determine effects of bacterial secondary metabolites on nodulation and phagocytosis, 10
514 potent chemicals were selected based on their common inhibitory activity on both phagocytosis

bioRxiv preprint doi: https://doi.org/10.1101/556159; this version posted February 20, 2019. The copyright holder for this preprint (which was not certified by peer review) is the author/funder, who has granted bioRxiv a license to display the preprint in perpetuity. It is made available under aCC-BY 4.0 International license.

and nodulation and their median inhibition concentration (IC_{50}) values were calculated. Percentages of phagocytosis against increasing concentrations of HB chemicals were calculated and their IC_{50} values were calculated using Probit analysis (https://probitanalysis.wordpress.com). To assess a competitive inhibitory activity between test compound and 5-HT, HB chemicals were injected in different doses (0, 0.01, 0.1, 1 and 10 μg/larva) along with a fixed 5-HT concentration (1 μg/larva) and FITC-tagged bacteria (500 cells/larva). In a separate experiment, different doses of 5-HT were injected into the larvae with a fixed HB compound content (1 μg/larva). At 15 min after bacterial injection, hemocytes from treated larvae were collected in ACB and phagocytosis assay was performed as described above.

Chemical derivatives and their inhibitory activities against Se-5HTR

Based on potent phenylethylamide (PEA) HB compounds, 45 additional PEA samples (S5 Fig) were obtained from Korea Chemical Bank of the Korea Research Institute of Chemical Technology (KRICT). Derivative compounds were dissolved in DMSO, diluted into desired concentrations with DMSO, and stored at -20°C. These PEA chemicals were then tested for their abilities to suppress nodule formation and phagocytosis in *S. exigua* as described above. For nodulation inhibition assay, each chemical (150 ng/larva) was injected into larval hemocoel along with bacterial suspension (~1.8×10^5 cfu/larva). Each treatment was triplicated independently using five insects for each replication. For phagocytosis inhibition assay, 5 μL of FITC-tagged *E. coli* suspension along with 150 ng of each chemical was injected into L5 larval hemocoel of *S. exigua*. After incubating for 15 min, hemocytes undergoing phagocytosis were counted using previously described method.

bioRxiv preprint doi: https://doi.org/10.1101/556159; this version posted February 20, 2019. The copyright holder for this preprint (which was not certified by peer review) is the author/funder, who has granted bioRxiv a license to display the preprint in perpetuity. It is made available under aCC-BY 4.0 International license.

538 **Chemical synthesis of PhX**

539 A potent chemical was designed as PhX ((*S*)-2-(1,4-dioxohexahydropyrrolo[1,2-*a*]pyrazin-
540 2(*1H*)-yl)-*N*-(4-methoxyphenethyl)acetamide) and chemically synthesized according to a method
541 described in S6 Fig.

542

543 **Statistical analysis**

544 All studies were triplicated independently. Results are expressed as mean ± standard error.
545 Results were plotted using Sigma plot (Systat Software, San Jose, CA, USA). Means were
546 compared by least squared difference (LSD) test of one-way analysis of variance (ANOVA)
547 using POC GLM of SAS program [71] and discriminated at Type I error = 0.05.

548

549 **Funding**

550 This work was supported by a grant (No. 2017R1A2133009815) of the National Research
551 Foundation (NRF) funded by the Ministry of Science, ICT and Future Planning, Republic of
552 Korea. This work was also supported by a project (No SI1808, Development of crop protection
553 agents leading the future market). The chemical library used in this research was provided by
554 Korea Chemical Bank (http://www.chembank.org) of the Korea Research Institute of Chemical
555 Technology (KRICT).

556

557 **Acknowledgments**

558 We appreciate Youngim Song for ordering and arranging materials and Malsook Cho for rearing
559 insects. Work in the Bode lab was supported by the LOEWE Center Translational Biodiversity
560 Genomics funded by the state of Hesse, Germany.

bioRxiv preprint doi: https://doi.org/10.1101/556159; this version posted February 20, 2019. The copyright holder for this preprint (which was not certified by peer review) is the author/funder, who has granted bioRxiv a license to display the preprint in perpetuity. It is made available under aCC-BY 4.0 International license.

561

562 **Author Contributions**

563 **Conceptualization**: Yonggyun Kim.

564 **Formal analysis**: Ariful Hasan, Yonggyun Kim.

565 **Investigation**: Hyun-Suk Yeom, Jaewook Ryu, Helge B. Bode, Yonggyun Kim.

566 **Project administration**: Yonggyun Kim.

567 **Supervision**: Hyun-Suk Yeom, Jaewook Ryu, Helge B. Bode, Yonggyun Kim.

568 **Writing – original draft**: Ariful Hasan, Yonggyun Kim.

569 **Writing – review & editing**: Ariful Hasan, Hyun-Suk Yeom, Jaewook Ryu, Helge B. Bode,

570 Yonggyun Kim.

571

bioRxiv preprint doi: https://doi.org/10.1101/556159; this version posted February 20, 2019. The copyright holder for this preprint (which was not certified by peer review) is the author/funder, who has granted bioRxiv a license to display the preprint in perpetuity. It is made available under aCC-BY 4.0 International license.

572 **References**

573

574 1. Roshchina VV. 2010. New trends and perspectives in the evolution of neurotransmitters in
575 microbial, plant, and animal cells. Adv Exp Med Biol. 2016;874:25-77.
576 2. Lovenberg W, Weissbach H, Udenfriend S. 1962. Aromatic L-amino acid decarboxylase. J
577 Biol Chem. 1962;237:89-93.
578 3. Hufton SE, Jennings IG, Cotton RG. Structure and function of the aromatic amino acid
579 hydroxylases. Biochem. J. 1995;311:353-66.
580 4. Roberts KM, Fitzpatrick PF. 2013. Mechanisms of tryptophan and tyrosine hydroxylase.
581 IUBMB Life 2013;65:350-357.
582 5. Zhang X, Beaulieu JM, Sotnikova TD, Gainetdinov RR, Caron MG. Tryptophan
583 hydroxylase-2 controls brain serotonin synthesis. Science. 2004;305:217.
584 6. Gershon MD, Tack J. The serotonin signaling system: from basic understanding to drug
585 development for functional GI disorders. Gastroenterology. 2007;132:397-414.
586 7. Richtand NM, McNamara RK. Serotonin and dopamine interactions in psychosis prevention.
587 Prog Brain Res. 2008;172:141-53.
588 8. Monti JM. Serotonin control of sleep-wake behavior. Sleep Med Rev. 2011;15:269-81.
589 9. Švob Štrac D, Pivac N, Mück-Šeler D. The serotonergic system and cognitive function.
590 Transl Neurosci. 2016;7:35-49.
591 10. Seuwen K, Pouysségur J. Serotonin as a growth factor. Biochem. Pharmacol. 1990;39:985-90.
592 11. Li N, Wallén NH, Ladjevardi M, Hjemdahl P. Effects of serotonin on platelet activation in
593 whole blood. Blood Coagul Fibrinolysis 1997;8:517-23.
594 12. Hayashi K, Fujita Y, Ashizawa T, Suzuki F, Nagamura Y, Hayano-Saito Y. Serotonin

bioRxiv preprint doi: https://doi.org/10.1101/556159; this version posted February 20, 2019. The copyright holder for this preprint (which was not certified by peer review) is the author/funder, who has granted bioRxiv a license to display the preprint in perpetuity. It is made available under aCC-BY 4.0 International license.

595 attenuates biotic stress and leads to lesion browning caused by a hypersensitive response to
596 *Magnaporthe oryzae* penetration in rice. Plant J. 2016;85:46-56.
597 13. Majeed ZR, Abdeljaber E, Soveland R, Cornwell K, Bankemper A, Koch F, et al. Modulatory
598 action by the serotonergic system: behavior and neurophysiology in *Drosophila*
599 *melanogaster*. Neural Plast. 2016;2016:1-23.
600 14. Huser A, Eschment M, Güllü N, Kan C, Böpple K, Pankevych L. et al. Anatomy and
601 behavioral function of serotonin receptors in *Drosophila melanogaster* larvae. PLoS One
602 2017;12:e0181865.
603 15. Becnel J, Johnson O, Luo J, Nässel DR, Nichols CD. The serotonin 5-HT_{7Dro} receptor is
604 expressed in the brain of *Drosophila*, and is essential for normal courtship and mating. PLoS
605 One 2011;6:e20800.
606 16. Yuan Q, Lin F, Zheng X, Sehgal A. Serotonin modulates circadian entrainment in *Drosophila*.
607 Neuron. 2005;47:115-27.
608 17. Nichols CD. 5-HT_2 receptors in *Drosophila* are expressed in the brain and modulate aspects
609 of circadian behaviors. Dev Neurobiol. 2007;67:752-63.
610 18. Yuan Q, Joiner WJ, Sehgal A. A sleep-promoting role for the *Drosophila* serotonin receptor
611 1A. Curr. Biol. 2006;16:1051-62.
612 19. Neckameyer WS, Coleman CM, Eadie S, Goodwin SF. Compartmentalization of neuronal
613 and peripheral serotonin synthesis in *Drosophila melanogaster*. Genes Brain Behav.
614 2007;6:756-69.
615 20. Dierick HA, Greenspan RJ. Serotonin and neuropeptide F have opposite modulatory effects
616 on fly aggression. Nat. Genet. 2007;39:678-82.
617 21. Kaplan DD, Zimmermann G, Suyama K, Meyer T, Scott MP. A nucleostemin family GTPase,

bioRxiv preprint doi: https://doi.org/10.1101/556159; this version posted February 20, 2019. The copyright holder for this preprint (which was not certified by peer review) is the author/funder, who has granted bioRxiv a license to display the preprint in perpetuity. It is made available under aCC-BY 4.0 International license.

NS3, acts in serotonergic neurons to regulate insulin signaling and control body size. Genes Dev. 2008;22:1877-93.

22. Qi YX, Huang J, Li MQ, Wu YS, Xia RY, Ye GY. Serotonin modulates insect hemocyte phagocytosis via two different serotonin receptors. Elife 2016;5:e12241.

23. Python F, Stocker RF. Immunoreactivity against choline acetyltransferase, gamma-aminobutyric acid, histamine, octopamine, and serotonin in the larval chemosensory system of *Drosophila melanogaster*. J. Comp. Neurol. 2002;453:157-67.

24. Dasari S, Cooper RL. Direct influence of serotonin on the larval heart of *Drosophila melanogaster*. J. Comp. Physiol. B 2006;176:349-57.

25. Rodriguez MVG, Campos AR. Role of serotonergic neurons in the *Drosophila* larval response to light. BMC Neurosci. 2009;10:66.

26. Barnes, N.M., Sharp, T., 1999. A review of central 5-HT receptors and their function. Neuropharmacology 38, 1083-1152.

27. Nichols DE, Nichols CD. Serotonin receptors. Chem Rev. 2008;108:1614-41.

28. Roth BL. The serotonin receptors□: from molecular pharmacology to human therapeutics. Humana Press, Totowa, New Jersey. 2006.

29. Thompson AJ, Lummis SCR. 5-HT_3 Receptors. Curr. Pharm. Des. 2006;12:3615-30.

30. Watanabe T, Sadamoto H, Aonuma H. Identification and expression analysis of the genes involved in serotonin biosynthesis and transduction in the field cricket *Gryllus bimaculatus*. Insect Mol Biol. 2011;20:619-35.

31. Ono H, Yoshikawa H. Identification of amine receptors from a swallowtail butterfly, *Papilio xuthus* L.: cloning and mRNA localization in foreleg chemosensory organ for recognition of host plants. Insect Biochem Mol Biol. 2004;34:1247-56.

bioRxiv preprint doi: https://doi.org/10.1101/556159; this version posted February 20, 2019. The copyright holder for this preprint (which was not certified by peer review) is the author/funder, who has granted bioRxiv a license to display the preprint in perpetuity. It is made available under aCC-BY 4.0 International license.

641 32. Vleugels R, Lenaerts C, Baumann A, Vanden BJ, Verlinden H. Pharmacological
642 characterization of a 5-HT_1-type serotonin receptor in the red flour beetle, *Tribolium*
643 *castaneum*. PLoS One 2013;8:e65052.
644 33. Troppmann B, Balfanz S, Baumann A, Blenau W. Inverse agonist and neutral antagonist
645 actions of synthetic compounds at an insect 5-HT_1 receptor. Br. J. Pharmacol.
646 2010;159:1450-62.
647 34. Guo X, Ma Z, Kang L. Serotonin enhances solitariness in phase transition of the migratory
648 locust. Front. Behav Neurosci. 2013;7:129.
649 35. Qi YX, Xia RY, Wu YS, Stanley D, Huang J, Ye GY. Larvae of the small white butterfly,
650 *Pieris rapae*, express a novel serotonin receptor. J Neurochem. 2014;131:767-77.
651 36. Qi YX, Jin M, Ni XY, Ye GY, Lee Y, Huang J. Characterization of three serotonin receptors
652 from the small white butterfly, *Pieris rapae*. Insect Biochem. Mol. Biol. 2017;87:107-16.
653 37. Thamm M, Balfanz S, Scheiner R, Baumann A, Blenau W. Characterization of the 5-HT_{1A}
654 receptor of the honeybee (*Apis mellifera*) and involvement of serotonin in phototactic
655 behavior. Cell Mol. Life Sci. 2010;67:2467-79.
656 38. Schlenstedt J, Balfanz S, Baumann A, Blenau W. Am5-HT_7: molecular and pharmacological
657 characterization of the first serotonin receptor of the honeybee (*Apis mellifera*). J
658 Neurochem. 2006;98:1985-98.
659 39. Berridge MJ, Patel N. Insect salivary glands - stimulation of fluid secretion by 5-
660 hydroxytryptamine and adenosine-3', 5'-monophosphate. Science. 1968;162:462-3.
661 40. Berridge MJ. The role of 5-hydroxytryptamine and cyclic AMP in the control of fluid
662 secretion by isolated salivary glands. J Exp Biol. 1970;53:171-86.
663 41. Vanhoenacker P, Haegeman G, Leysen JE. 5-HT_7 receptors: current knowledge and future

bioRxiv preprint doi: https://doi.org/10.1101/556159; this version posted February 20, 2019. The copyright holder for this preprint (which was not certified by peer review) is the author/funder, who has granted bioRxiv a license to display the preprint in perpetuity. It is made available under aCC-BY 4.0 International license.

664 prospects. Trends Pharmacol. Sci. 2000;21:70-7.

665 42. Molaei G, Lange AB. The association of serotonin with the alimentary canal of the African
666 migratory locust, *Locusta migratoria*: distribution, physiology and pharmacological profile.
667 J Insect Physiol. 2003;49:1073-182.

668 43. Baines D, DeSantis T, Downer RGH. Octopamine and 5-hydroxytryptamine enhance the
669 phagocytic and nodule formation activities of cockroach (*Periplaneta americana*)
670 haemocytes. J Insect Physiol. 1992;38:905-14.

671 44. Kim K, Madanagapol N, Lee D, Ki Y. Octopamine and 5-hydroxytryptamine mediate
672 hemocytic phagocytosis and nodule formation via eicosanoids in the beet armyworm,
673 *Spodoptera exigua*. Arch. Insect Biochem. Physiol. 2009;90:162-76.

674 45. Kim GS, Kim Y. Up-regulation of circulating hemocyte population in response to bacterial
675 challenge is mediated by octopamine and 5-hydroxytryptamine via Rac1 signal in
676 *Spodoptera exigua*. J. Insect Physiol. 2010;56:559-66.

677 46. Kim Y, Ji D, Cho S, Park Y. Two groups of entomopathogenic bacteria, *Photorhabdus* and
678 *Xenorhabdus*, share an inhibitory action against phospholipase A_2 to induce host
679 immunodepression. J Invertebr Pathol. 2005;89: 258-64.

680 47. Shi YM, Bode HB. Chemical language and warfare of bacterial natural products in bacteria-
681 nematode-insect interactions. Nat Prod Rep 2018;35:309-35.

682 48. Tobias NJ, Shi YM, Bode HB. Refining the natural product repertoire in entomopathogenic
683 bacteria. Trends Microbiol. 2018;26:833-40.

684 49. Barak LS, Tiberi M, Freedman NJ, Kwatra MM, Lefkowitz RJ, Caron MG. A highly
685 conserved tyrosine residue in G protein-coupled receptors is required for agonist-mediated
686 ß2-adrenergic receptor sequestration. J Biol Chem 1994;269:2790-5.

bioRxiv preprint doi: https://doi.org/10.1101/556159; this version posted February 20, 2019. The copyright holder for this preprint (which was not certified by peer review) is the author/funder, who has granted bioRxiv a license to display the preprint in perpetuity. It is made available under aCC-BY 4.0 International license.

687 50. Ji TH, Grossmann M, Ji I. G protein-coupled receptors. I. Diversity of receptor-ligand
688 interactions. J Biol Chem. 1998;273:17299-302.
689 51. Huang ES. Construction of a sequence motif characteristic of aminergic G protein-coupled
690 receptors. Protein Sci. 2003;12:1360-67.
691 52. Park J, Stanley D, Kim Y. Rac1 mediates cytokine-stimulated hemocyte spreading via
692 prostaglandin biosynthesis in the beet armyworm, *Spodoptera exigua*. J Insect Physiol.
693 2013;59:682-9.
694 53. Venkatakrishnan AJ, Deupi X, Lebon G, Tate CG, Schertler GF, Babu MM. Molecular
695 signatures of G-protein-coupled receptors. Nature 2013;494:185-94.
696 54. Ho BY, Karschin A, Branchek T, Davidson N, Lester HA. The role of conserved aspartate
697 and serine residues in ligand binding and in function of the 5-HT_{1A} receptor: A site-directed
698 mutation study. FEBS Lett. 1992;312:259-62.
699 55. Shapiro DA, Kristiansen K, Weiner DM, Kroeze WK, Roth BL. Evidence for a model of
700 agonist-induced activation of 5-hydroxytryptamine 2A serotonin receptors that involves the
701 disruption of a strong ionic interaction between helices 3 and 6. J. Biol. Chem.
702 2002;277:11441-9.
703 56. Qanbar R, Bouvier M. Role of palmitoylation/depalmitoylation reactions in G-protein-
704 coupled receptor function. Pharmacol. Ther. 2003;97:1-33.
705 57. Romero G, von Zastrow M, Friedman PA. Role of PDZ proteins in regulating trafficking,
706 signaling, and function of GPCRs: means, motif, and opportunity. Adv Pharmacol.
707 2011;62:279-314.
708 58. Guseva D, Wirth A, Ponimaskin E. Cellular mechanisms of the 5-HT_7 receptor-mediated
709 signaling. Front. Behav. Neurosci. 2014;8:306.

bioRxiv preprint doi: https://doi.org/10.1101/556159; this version posted February 20, 2019. The copyright holder for this preprint (which was not certified by peer review) is the author/funder, who has granted bioRxiv a license to display the preprint in perpetuity. It is made available under aCC-BY 4.0 International license.

59. Choi C, Helfman DM. The Ras-ERK pathway modulates cytoskeleton organization, cell motility and lung metastasis signature genes in MDA-MB-231 LM2. Oncogene 2014;33:3668-76.

60. Papenfort K, Bassler BL. Quorum sensing signal-response systems in Gram-negative bacteria. Nat. Rev. Microbiol. 2016;14:576-88.

61. Bode E, He Y, Vo TD, Schultz R, Kaiser M, Bode HB. Biosynthesis and function of simple amides in *Xenorhabdus doucetiae*. Environ. Microbiol. 2017;19:4564-75.

62. Reimer D, Nollmann FI, Schultz K, Kaiser M, Bode HB. Xenortide biosynthesis by entomopathogenic *Xenorhabdus nematophila*. J Nat Prod. 2014;77:1976-80.

63. Bloudoff K, Schmeing TM. Structural and functional aspects of the nonribosomal peptide synthetase condensation domain superfamily: discovery, dissection and diversity. Biochim Biophys Acta 2017;1865:1587-604.

64. Proschak A, Zhou Q, Schöner T, Thanwisai A, Kresovic D, Dowling A, et al. Biosynthesis of the insecticidal xenocyloins in *Xenorhabdus bovienii*. Chembiochem. 2014;15:369-72.

65. Li J, Chen G, Webster JM. Nematophin, a novel antimicrobial substance produced by *Xenorhabdus nematophilus* (Enterobactereaceae). Can J Microbiol. 1997;43:770-3.

66. Nollmann FI, Dauth C, Mulley G, Kegler C, Kaiser M, Waterfield NR. et al. Insect-specific production of new GameXPeptides in *Photorhabdus luminescens* TTO1, widespread natural products in entomopathogenic bacteria. Chembiochem. 2015;16:205-8.

67. Cai M, Li Z, Fan F, Huang Q, Shao X, Song G. Design and synthesis of novel insecticides based on the serotonergic ligand 1-[(4-Aminophenyl) ethyl]-4-[3-(trifluoromethyl) phenyl] piperazine (PAPP). J Agric Food Chem. 2009;58:2624-9.

68. Verlinden H, Vleugels R, Broeck JV. Serotonin, serotonin receptors and their actions in

bioRxiv preprint doi: https://doi.org/10.1101/556159; this version posted February 20, 2019. The copyright holder for this preprint (which was not certified by peer review) is the author/funder, who has granted bioRxiv a license to display the preprint in perpetuity. It is made available under aCC-BY 4.0 International license.

733 insects. Neurotransmitter. 2015;2:e314

734 69. Shrestha S, Stanley D, Kim Y. PGE_2 induces oenocytoid cell lysis via a G protein-coupled
735 receptor in the beet armyworm, *Spodoptera exigua*. J. Insect Physiol. 2011; 57:1568-76.

736 70. Bustin SA, Benes V, Garson JA, Hellemans J, Huggett J, Kubista M, et al. The MIQE
737 guidelines: minimum information for publication of quantitative real-time PCR experiments.
738 Clin. Chem. 2009;55:4.

739 71. SAS Institute. SAS/STAT user's guide. SAS Institute, Inc., Cary, NC. 1989.

bioRxiv preprint doi: https://doi.org/10.1101/556159; this version posted February 20, 2019. The copyright holder for this preprint (which was not certified by peer review) is the author/funder, who has granted bioRxiv a license to display the preprint in perpetuity. It is made available under aCC-BY 4.0 International license.

740 **Figure captions**

741

742 **Fig. 1. Bioinformatics analysis of a novel 5-HTR$_7$ identified from *S. exigua* (Se-5HTR:**
743 **MH025798). (A)** Phylogenetic analysis of 5HTRs. Amino acid sequences were retrieved from
744 GenBank: Hs5HTR1D (NP_000855.1), Ss5HTR1D (NP_999323.1), Rn5HTR1D
745 (NP_036984.1), Oc5HTR1D (NP_001164624.1), NP_000854.1 Hs5HTR1B (NP_000854.1),
746 Dr5HTR1D (NP_001139158.1), Hs5HTR1F (NP_000857.1), Hs5HTR1E (NP_000856.1),
747 Cp5HTR1E (NP_001166222.1), Hs5HTR1A (NP_000515.2), Ap5HTR1B (ABY85411.1),
748 Ms5HTR (ABI33827.1), Pr5HTR1B (XP_022120028.1), Am5HTR1 (NP_001164579.1),
749 Dm5HTR1B (NP_001163201.2), Pa5HTR1 (CAX65666.1), Pr5HTR1A (XP_022129638.1),
750 Ap5HTR1A (ABY85410.1), Hs5HTR7 (P34969), Rn5HTR7 (P32305), Pr5HTR7
751 (AMQ67549.1), Am5HTR7 (NP_001071289.1), Dm5HTR7 (NP_524599.1), Ae5HTR7
752 (Q9GQ54), Hs5HTR4 (Q13639), Cp5HTR4 (O70528), Rn5HTR4 (Q62758), Mm5HTR4
753 (P97288), Hs5HTR6 (P50406), Pt5HTR6 (Q5IS65), It5HTR6 (XP_005317590.1), Rn5HTR6
754 (P31388), Mm5HTR6 (Q9R1C8), Cp5HTR6 (XP_003471412.1), Pm5HTR2A (KPJ17794.1),
755 Pr5HTR2A (XP_022112310.1), Bm5HTR2A (NP_001296483.1), Cl5HTR2A
756 (XP_014254278.1), Rp5HTr2B (AKQ13312.1), Mq5HTR2A (KOX78271.1), Am5HTr2B
757 (NP_001189389.1), Hs5HTR2A (NP_000612.1), Hs5HTR2C (NP_000859.1), Hs5HTR2B
758 (NP_000858.3), Pt5HTR2C (XP_015921531.1), Mp5HTR2C (XP_022169104.1), Am5HTr2A
759 (NP_001191178.1), Pr5HTR2C (XP_022122944.1), Ba5HTR2C (XP_023955125.1),
760 Rn5HTR5B (P35365), Mm5HTR5B (P31387), Hs5HTR5A (NP_076917.1), Rn5HTR5A
761 (P35364), Mm5HTR5A (P30966), Hs5HTR3C (NP_570126.2), Hs5HTR3E (NP_001243542.1),
762 Hs5HTR3D (NP_001157118.1), Hs5HTR3B (NP_006019.1), Rn5HTR3B (NP_071525.1),

bioRxiv preprint doi: https://doi.org/10.1101/556159; this version posted February 20, 2019. The copyright holder for this preprint (which was not certified by peer review) is the author/funder, who has granted bioRxiv a license to display the preprint in perpetuity. It is made available under aCC-BY 4.0 International license.

763 Hs5HTR3A (AP35868.1), Cp5HTR3A (O70212), Rn5HTR3A (NP_077370.2), Mm5HTR3A
764 (P23979). The phylogenetic tree was constructed using neighbor-joining method. Bootstrap
765 values on branch nodes were obtained after 1,000 repetitions. **(B)** Amino acid sequence
766 alignment of Se-5HTR with orthologous receptors from *Homo sapiens* (Hs-5HTR7: P34969),
767 *Drosophila melanogaster* (Dm-5HTR7: NP_524599.1), *Manduca sexta* (Ms-5HTR7:
768 AGL46976.1), and *Pieris rapae* (Pr-5HTR7: AMQ67549.1). Identical residues among these five
769 sequences are illustrated as white letters against black. Dashes within sequences indicate gaps
770 introduced to maximize homology. Putative seven transmembrane domains (TM1-TM7) are
771 shown as blue bars. Potential N-glycosylation sites (), potential phosphorylation sites for
772 protein kinase A and/or C (), potential residue to interacts with 5-HT amino group () and 5-
773 HT hydroxyl group (), potential disulfide bond groups (), and potential post translational
774 palmitoylation sites () are indicated. Overbars indicate unique motif to aminergic receptor,
775 agonist mediated sequestration and resensitization motif, and PDZ-domain binding motif,
776 respectively. Conserved domains were determined using InterPro tool
777 (https://www.ebi.ac.uk/interpro/) and Prosite (http://prosite.expasy.org/) whereas other residues
778 and motifs were predicted using several tools from DTU bioinformatics
779 (www.cbs.dtu.dk/services/).
780
781 **Fig. 2. Expression profile of *Se-5HTR*. (A)** Differential expression of *Se-5HTR* in different
782 developmental stages: egg, larval instars ('L1-L5'), pupa ('Pu'), and adult ('Ad'). **(B)**
783 Differential expression of *Se-5HTR* in different tissues of L5 larvae: hemocyte ('HC), midgut
784 ('GUT'), fat body ('FB'), and brain ('BR'). **(C)** Expression pattern of *Se-5HTR* in immune-
785 challenged L5 larvae: *Escherichia coli* ('Ec'), *Xenorhabdus nematophila* ('Xn'), *Photorhabdus*

bioRxiv preprint doi: https://doi.org/10.1101/556159; this version posted February 20, 2019. The copyright holder for this preprint (which was not certified by peer review) is the author/funder, who has granted bioRxiv a license to display the preprint in perpetuity. It is made available under aCC-BY 4.0 International license.

786 *temperata temperata* ('Ptt'), *Serratia marcescens* ('Sm'), and *Beauveria bassiana* ('Bb').
787 Immune challenge was performed by injecting each L5 larva with 1.8×10^5 cells of bacteria or 5
788 $\times 10^5$ conidia of fungi. After incubation at 25°C for 8 h, gene expression analysis was performed
789 using RT-PCR and RT-qPCR. As a constitutive expressional control, a ribosomal gene, *RL32*,
790 was used for expression analysis in RT-PCR and RT-qPCR. Each measurement was replicated
791 three times with independent biological samples. Histogram bars annotated with the same letter
792 are not significantly different at Type I error = 0.05 (LSD test).
793
794 **Fig. 3. Effect of an inhibitor specific to 5-HT$_7$ receptor ('SB-269970') on hemocyte**
795 **behaviors of *S. exigua*. (A)** Total hemocyte count (THC) analysis in L5 larvae. For the assay, 2
796 µg of 5-HT or 2 µg of SB-269970 was injected. THC was assessed with or without bacterial co-
797 injection (1.8×10^5 cells per larva). **(B)** Hemocyte-spreading behavior analysis. Hemocyte-
798 spreading was assessed with a 20 µL reaction mixture containing 1 or 2 µL test chemical with 18
799 or 19 µL hemocytes. 5-HT was co-applied with SB-269970 at ratios of 1:10 (2 µg 5-HT: 20 µg
800 SB-269970) and 10:1 (20 µg 5-HT: 2 µg SB-269970). Spread cells were stained with F-actin and
801 FITC-labeled phalloidin. Nuclei were stained with DAPI. Each treatment was independently
802 replicated three times. Histogram bars indicate percentages of spread hemocytes and error bars
803 indicate standard deviation. Histogram bars annotated with the same letter are not significantly
804 different at Type I error = 0.05 (LSD test).
805
806 **Fig. 4. RNA interference (RNAi) of *Se-5HTR* and suppression of hemocyte behaviors. (A)**
807 RNAi of *Se-5HTR* expression with a gene-specific dsRNA (dsSe-5HTR). About 900 ng of dsSe-
808 5HTR was injected to L5. At 0, 12, 24, and 48 h post-injection (PI), expression levels of *Se-*

bioRxiv preprint doi: https://doi.org/10.1101/556159; this version posted February 20, 2019. The copyright holder for this preprint (which was not certified by peer review) is the author/funder, who has granted bioRxiv a license to display the preprint in perpetuity. It is made available under aCC-BY 4.0 International license.

809 *5HTR* were assessed from whole body. Expression levels of *Se-5HTR* in different tissue parts
810 were assessed at 24 h PI. As a constitutive expressional control, a ribosomal gene, *RL32*, was
811 used for expression analysis in RT-PCR and RT-qPCR. As a control RNAi (dsCON), dsRNA
812 specific to *CpBV-ORF302* (a viral gene) was used for expression analysis. In RT-qPCR, each
813 treatment was triplicated. **(B)** Influence of RNAi on up-regulation of total hemocyte count (THC)
814 in response to bacterial challenge. At 24 h PI of dsSe-5HTR, hemolymph was collected from L5
815 larvae for THC assessment. Each treatment was replicated three times. **(C)** Influence of RNAi on
816 hemocyte-spreading behavior. For spreading assay, hemocytes from larvae treated with dsRNA
817 were collected at 24 h. Each treatment was independently replicated three times. Spread cells
818 were stained with F-actin and FITC-labeled phalloidin. Nuclei were stained with DAPI.
819 Histogram bars indicate percentages of spread hemocytes and error bars indicate standard
820 deviation. Different letters above standard error bars indicate significant difference among means
821 at type I error = 0.05 (LSD test). Asterisks represent significant difference between control and
822 treatment in each tissue.
823
824 **Fig. 5. RNA interference (RNAi) of *Se-5HTR* and suppression of cellular immune responses.**
825 **(A)** Analysis of phagocytosis in L5 larvae of *S. exigua*. FITC-tagged *E. coli* were injected into
826 L5 larvae at 24 h post-injection of dsSe-5HTR. A specific inhibitor (SB-269970) to 5-HT_7
827 receptor was co-injected at a dose of 2 μg along with FITC-tagged bacteria. At 15 min after
828 injection, phagocytic cells were observed under a fluorescent microscope at 400 × magnification
829 and percentage of phagocytotic hemocytes was calculated from randomly chosen 100 cells. Total
830 hemocytes were observed from bright-field ('BF'). Each treatment was independently replicated
831 three times. **(B)** Nodulation assay. After RNAi, *E. coli* (1.8×10^5 cells/larva) was injected to L5

bioRxiv preprint doi: https://doi.org/10.1101/556159; this version posted February 20, 2019. The copyright holder for this preprint (which was not certified by peer review) is the author/funder, who has granted bioRxiv a license to display the preprint in perpetuity. It is made available under aCC-BY 4.0 International license.

832 larvae. SB-269970 (2 μg/larva) was co-injected with bacteria. After 8 h incubation at 25°C,
833 treated insects were assessed for nodule formation. Histogram bars indicate percentages of
834 phagocytosis and error bars indicate standard deviation. Histogram bars annotated with the same
835 letter are not significantly different at Type I error = 0.05 (LSD test).
836
837 **Fig. 6. Immunosuppressive activities of organic extracts from culture broth of**
838 ***Xenorhabdus nematophila* ('Xn') and *Photorhabdus temperata temperata* ('Ptt') bacteria**
839 **against L5 larvae of *S. exigua*.** Each larva was injected with *E. coli* (10^5 cells) along with 1 μL
840 of ethyl acetate ('EAX') or butanol ('BX') extract. **(A)** Phagocytosis in L5 larvae. FITC-tagged
841 *E. coli* were injected to L5 larvae at 24 h post-injection of an organic extract. After 15 min,
842 phagocytic cells were observed under a fluorescent microscope at 400 × magnification and
843 percentage of phagocytotic hemocytes was calculated from randomly chosen 100 cells. Each
844 treatment was independently replicated three times. **(B)** Nodule formation. *E. coli* (1.8×10^5
845 cells/larva) was injected to L5 larvae. An organic extract was co-injected with the bacteria. After
846 8 h of incubation at 25°C, treated insects were assessed for nodule formation. Each treatment
847 was replicated with 10 larvae. Different letters above standard deviation bars indicate significant
848 difference among means at Type I error = 0.05 (LSD test).
849
850 **Fig. 7. Screening 37 bacterial secondary metabolites derived from *X. nematophila* and *P.***
851 ***temperata temperata* for their effects on cellular immune responses mediated by Se-5HTR in**
852 ***S. exigua*. (A)** Screening with phagocytosis assay. FITC-tagged *E. coli* cells were injected to L5
853 larvae along with 1 μg of each test chemical. After 15 min, phagocytic cells were observed under
854 a fluorescent microscope at 400 × magnification and percentage of phagocytotic hemocytes was

bioRxiv preprint doi: https://doi.org/10.1101/556159; this version posted February 20, 2019. The copyright holder for this preprint (which was not certified by peer review) is the author/funder, who has granted bioRxiv a license to display the preprint in perpetuity. It is made available under aCC-BY 4.0 International license.

855 calculated from randomly chosen 100 cells. Each treatment was independently replicated three
856 times. **(B)** Screening with nodule formation assay. *E. coli* (1.8×10^5 cells/larva) was injected to
857 L5 larvae along with 1 µg of each test chemical. After 8 h of incubation at 25°C, treated insects
858 were assessed for nodule formation. Each treatment was replicated with 10 larvae. Asterisks
859 above standard deviation bars indicate significant difference compared to control ('CON'
860 without inhibitor) at Type I error = 0.05 (*), 0.01 (**), and 0.005 (***) (LSD test).
861
862 **Fig. 8. Competitive inhibition of 10 selected bacterial metabolites derived from *X.***
863 ***nematophila* and *P. temperata temperata* with 5-HT against Se-5HTR mediating**
864 **phagocytosis.** FITC-tagged *E. coli* cells were injected to L5 larvae along with test chemicals.
865 After 15 min, phagocytic cells were observed under a fluorescent microscope at 400 ×
866 magnification and percentage of phagocytotic hemocytes was calculated from randomly chosen
867 100 cells. Each treatment was independently replicated three times. **(A)** Dose-response of
868 inhibitory compound (0, 0.01, 0.1, 1, and 10 µg/larva) with a fixed 5-HT concentration (1
869 µg/larva). **(B)** Dose-response of 5-HT (0, 0.02, 0.2, 2 and 20 µg/larva) with a fixed HB
870 compound concentration (1 µg/larva). 'CON' represents a positive control without any inhibitor.
871
872 **Fig. 9. Validation of phenylethylamide (PEA) compounds for their inhibitory activities**
873 **against 5-HTR using derivatives with different side chains ('X' and 'Y' of PEA skeleton). (A)**
874 Screening of 45 PEA derivatives for their effects on hemocyte phagocytosis of *S. exigua* with HB
875 44, a potent bacterial metabolite, as reference. PEA compounds (300 ng/larva) were injected into
876 hemocoels of L5 larvae along with FITC-tagged bacteria. After incubating for 15 min,
877 hemocytes were assessed for phagocytosis. Asterisks above standard deviation bars indicate

bioRxiv preprint doi: https://doi.org/10.1101/556159; this version posted February 20, 2019. The copyright holder for this preprint (which was not certified by peer review) is the author/funder, who has granted bioRxiv a license to display the preprint in perpetuity. It is made available under aCC-BY 4.0 International license.

878 significant difference compared to control ('CON' without inhibitor) at Type I error = 0.05 (*),
879 0.01 (**), and 0.005 (***) (LSD test). **(B)** Chemical structures of three selected PEA compounds
880 and their median inhibitory doses (IC_{50}). **(C)** Competitive inhibition of the three selected PEA
881 derivatives with 5-HT against Se-5HTR mediated phagocytosis. For dose-response analysis of
882 inhibitory compounds (0, 0.3, 3, 30, and 300 ng/larva), a fixed 5-HT concentration (1 µg/larva)
883 was used. For dose-response of 5-HT (0, 2, 20, 200 and 2,000 ng/larva), a fixed HB compound
884 concentration (1 µg/larva) was used. 'CON' represents a positive control without any inhibitor.
885
886 **Fig. 10. Specific inhibition of a designed compound (PhX) on Se-5HTR with a commercial**
887 **5-HTR$_7$ inhibitor (SB-269970) as reference in phagocytosis of *S. exigua*.** FITC-tagged *E. coli*
888 cells were injected to L5 larvae along with test chemicals. After 15 min, phagocytic cells were
889 observed under a fluorescent microscope at 400 × magnification and percentage of phagocytotic
890 hemocytes was calculated from randomly chosen 100 cells. Each treatment was independently
891 replicated three times. **(A)** Dose-response of PhX and SB-269970 with a fixed 5-HT
892 concentration (500 ng/larva). **(B)** Dose-response of 5-HT (0, 0.002, 0.02, 0.2, and 2 µg/larva)
893 with a fixed inhibitor concentration (10 ng/larva). 'CON' represents a positive control without
894 any inhibitor.

bioRxiv preprint doi: https://doi.org/10.1101/556159; this version posted February 20, 2019. The copyright holder for this preprint (which was not certified by peer review) is the author/funder, who has granted bioRxiv a license to display the preprint in perpetuity. It is made available under aCC-BY 4.0 International license.

(A)

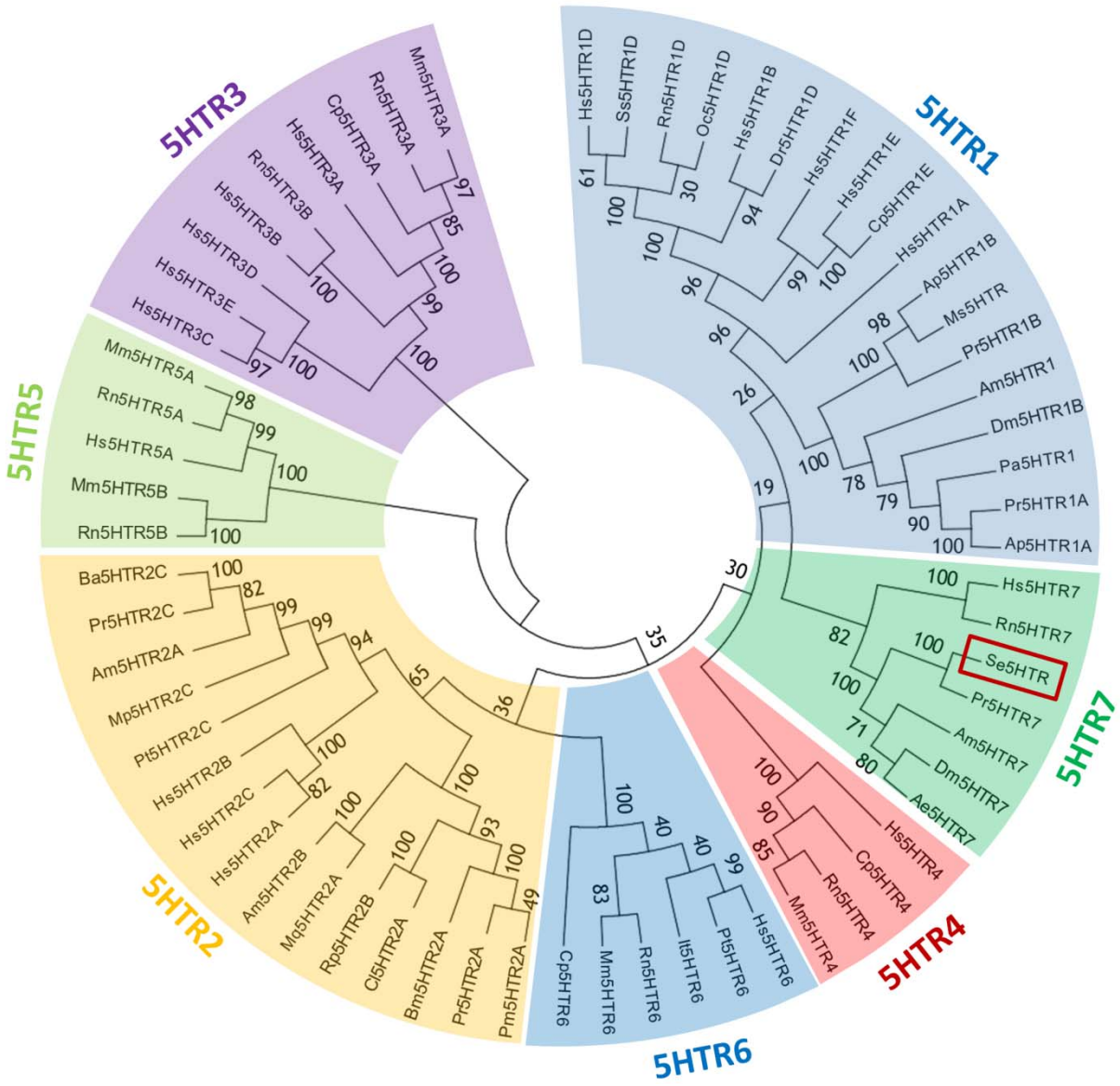

bioRxiv preprint doi: https://doi.org/10.1101/556159; this version posted February 20, 2019. The copyright holder for this preprint (which was not certified by peer review) is the author/funder, who has granted bioRxiv a license to display the preprint in perpetuity. It is made available under aCC-BY 4.0 International license.

(B)

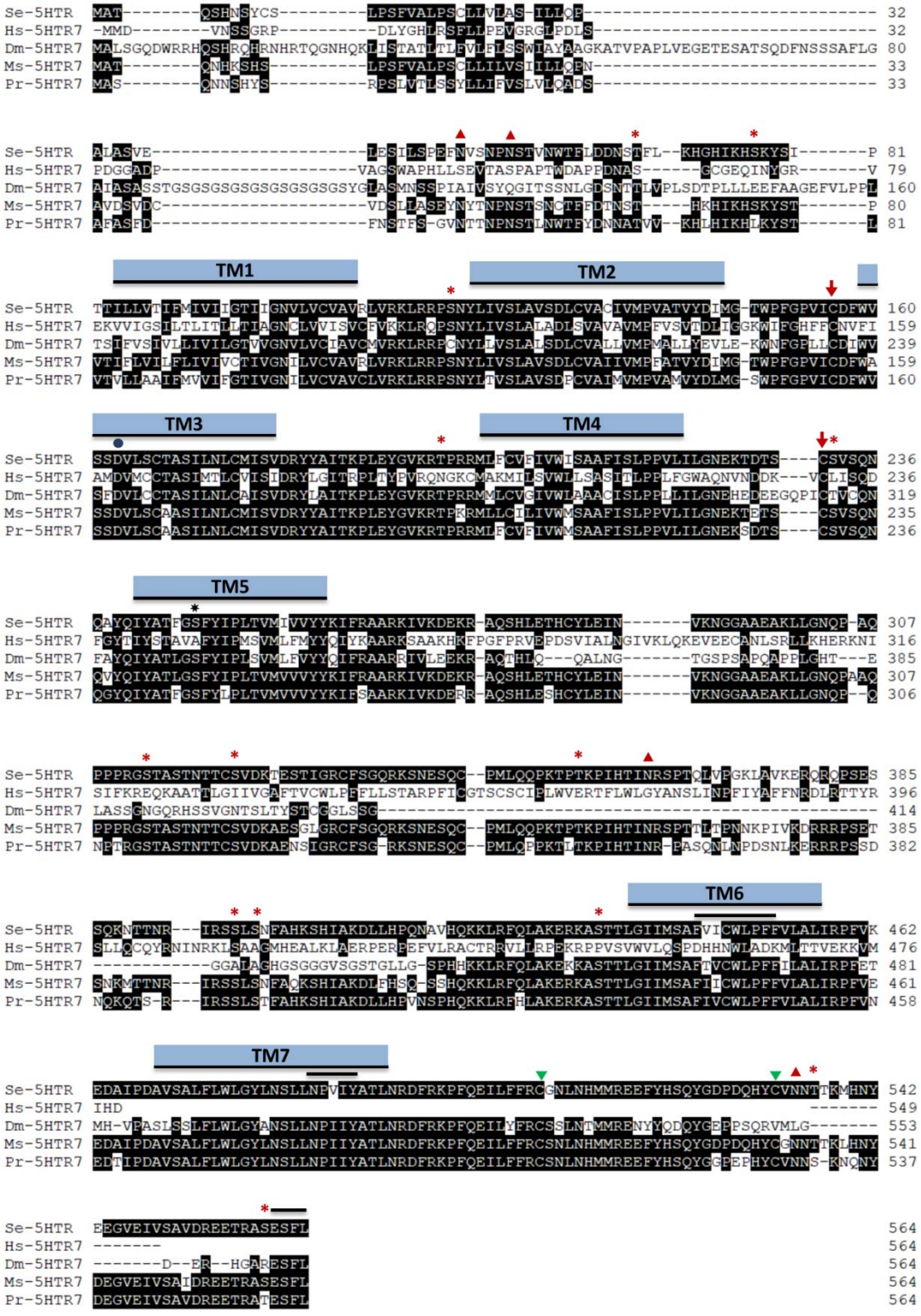

Fig. 1

bioRxiv preprint doi: https://doi.org/10.1101/556159; this version posted February 20, 2019. The copyright holder for this preprint (which was not certified by peer review) is the author/funder, who has granted bioRxiv a license to display the preprint in perpetuity. It is made available under aCC-BY 4.0 International license.

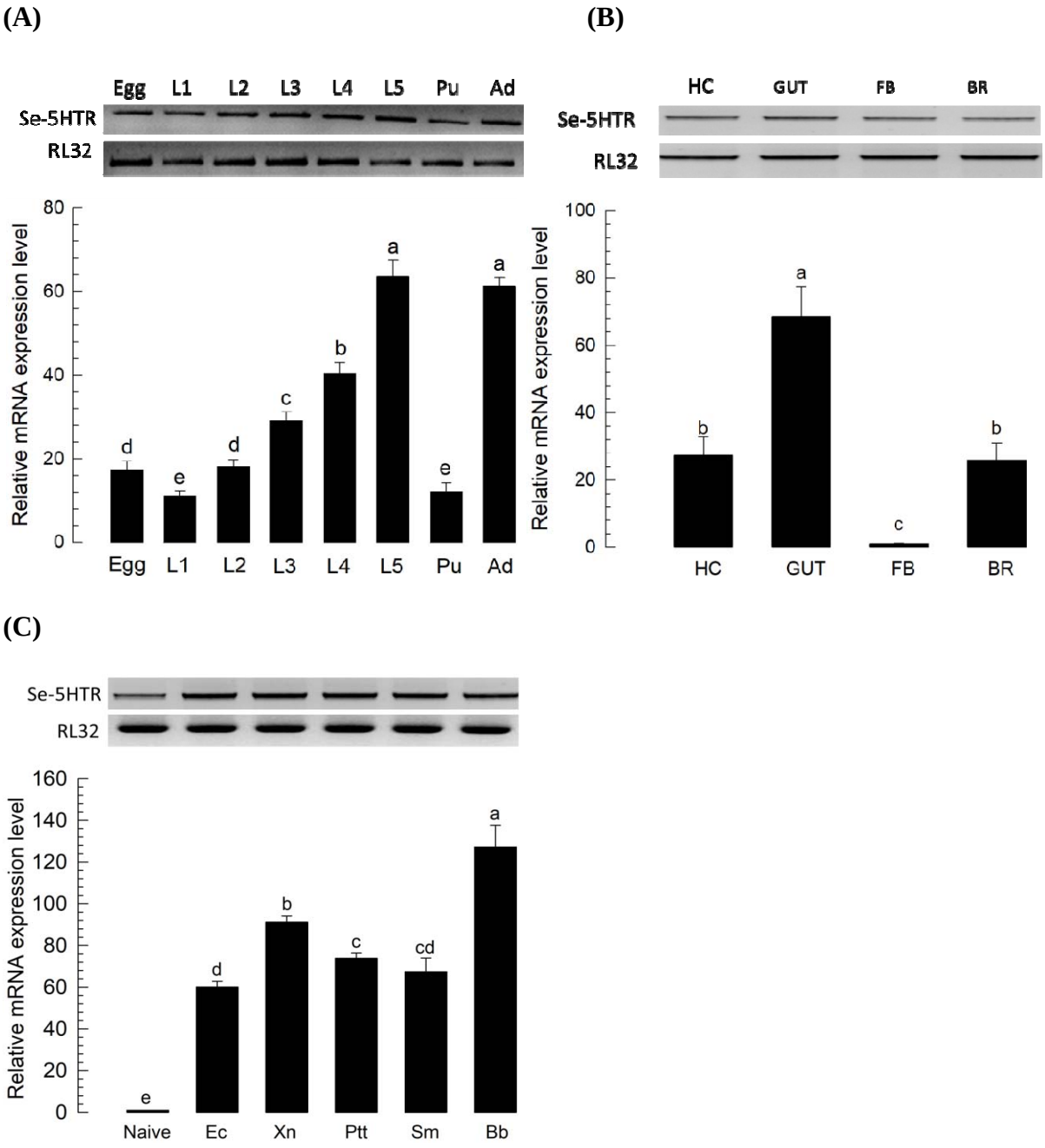

Fig. 2

bioRxiv preprint doi: https://doi.org/10.1101/556159; this version posted February 20, 2019. The copyright holder for this preprint (which was not certified by peer review) is the author/funder, who has granted bioRxiv a license to display the preprint in perpetuity. It is made available under aCC-BY 4.0 International license.

(A)

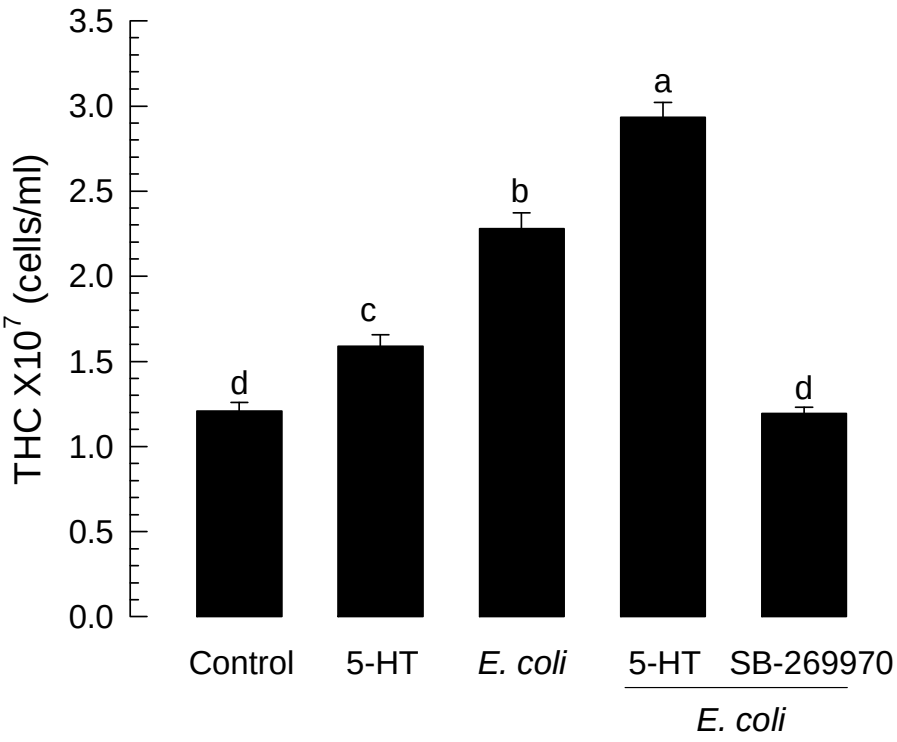

bioRxiv preprint doi: https://doi.org/10.1101/556159; this version posted February 20, 2019. The copyright holder for this preprint (which was not certified by peer review) is the author/funder, who has granted bioRxiv a license to display the preprint in perpetuity. It is made available under aCC-BY 4.0 International license.

(B)

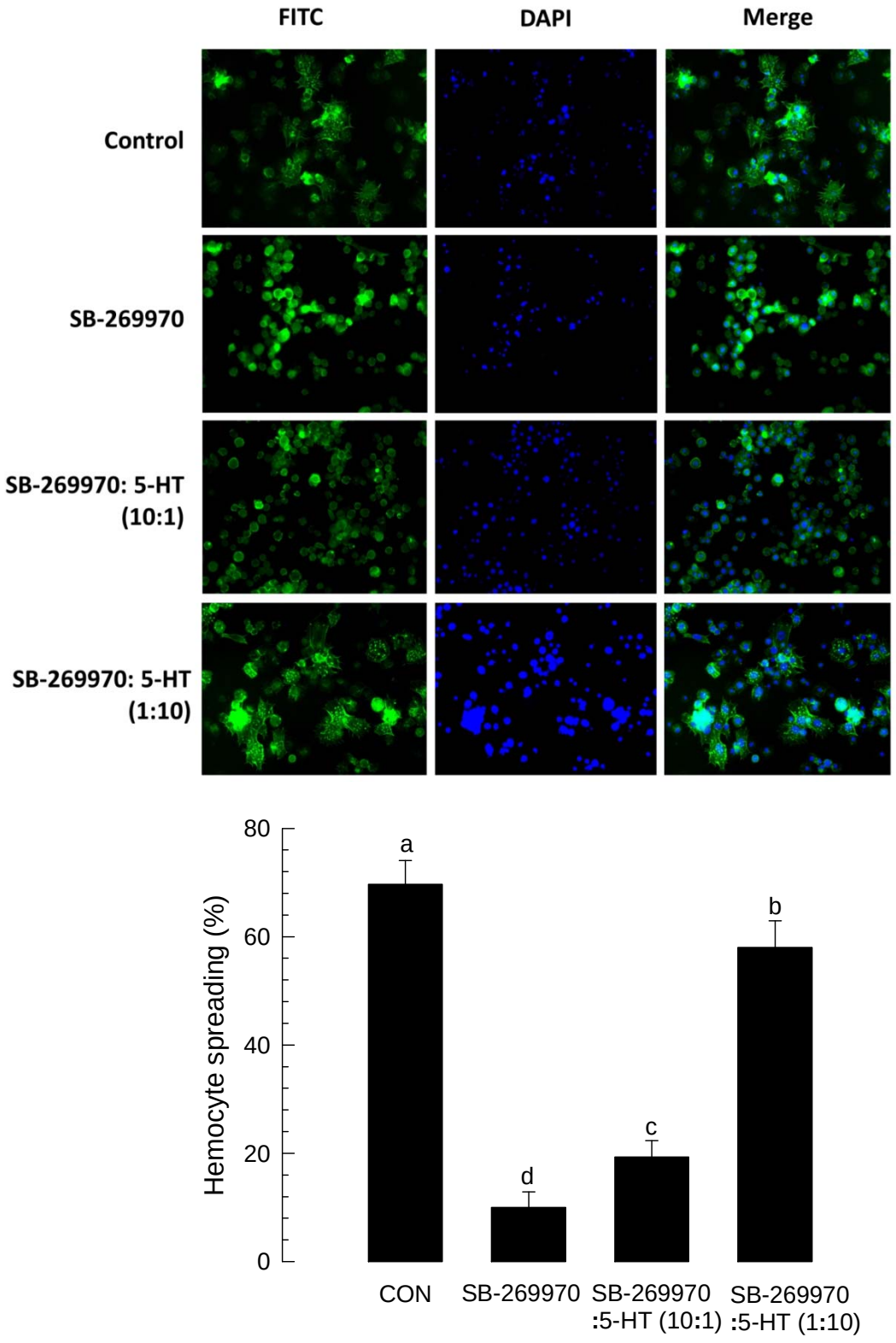

Fig. 3

bioRxiv preprint doi: https://doi.org/10.1101/556159; this version posted February 20, 2019. The copyright holder for this preprint (which was not certified by peer review) is the author/funder, who has granted bioRxiv a license to display the preprint in perpetuity. It is made available under aCC-BY 4.0 International license.

(A)

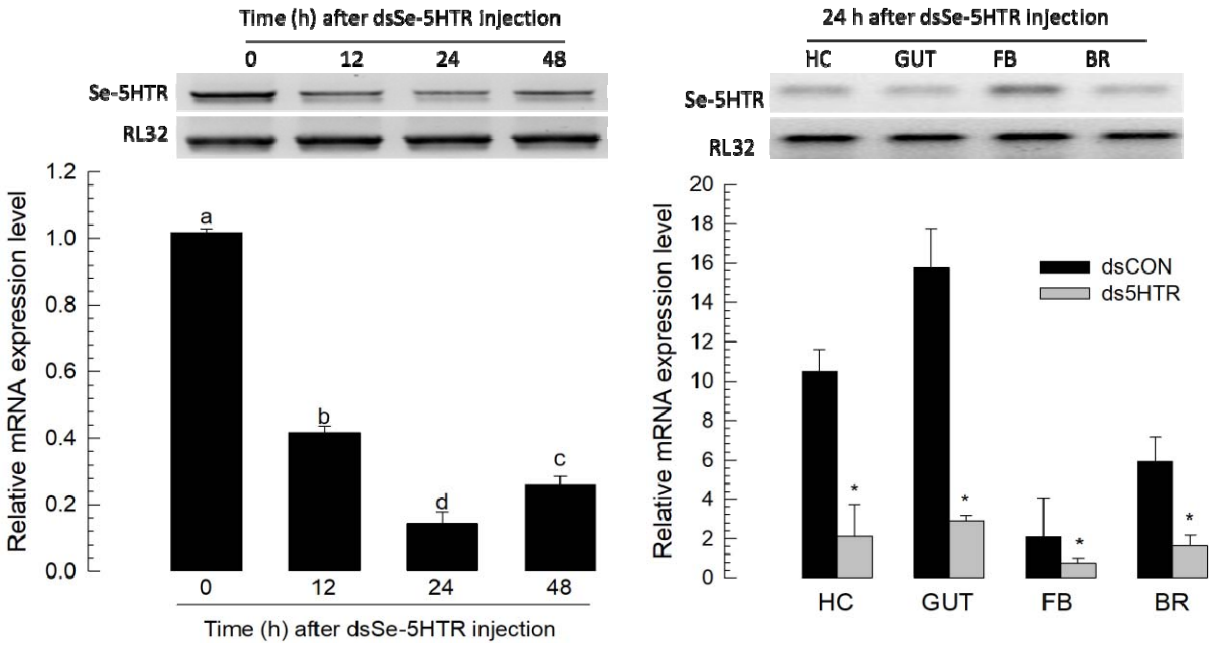

(B)

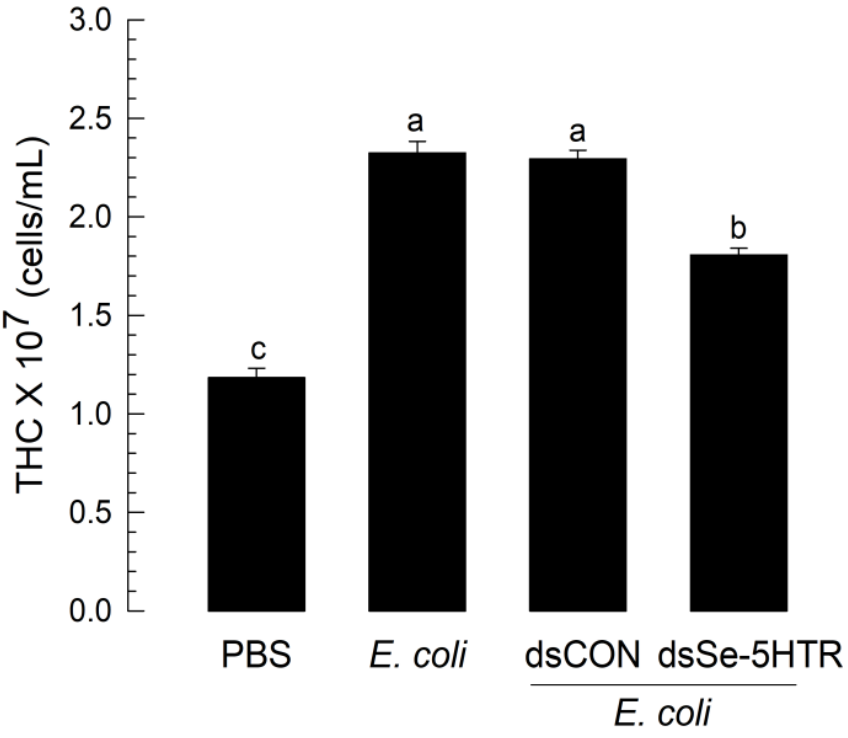

bioRxiv preprint doi: https://doi.org/10.1101/556159; this version posted February 20, 2019. The copyright holder for this preprint (which was not certified by peer review) is the author/funder, who has granted bioRxiv a license to display the preprint in perpetuity. It is made available under aCC-BY 4.0 International license.

(C)

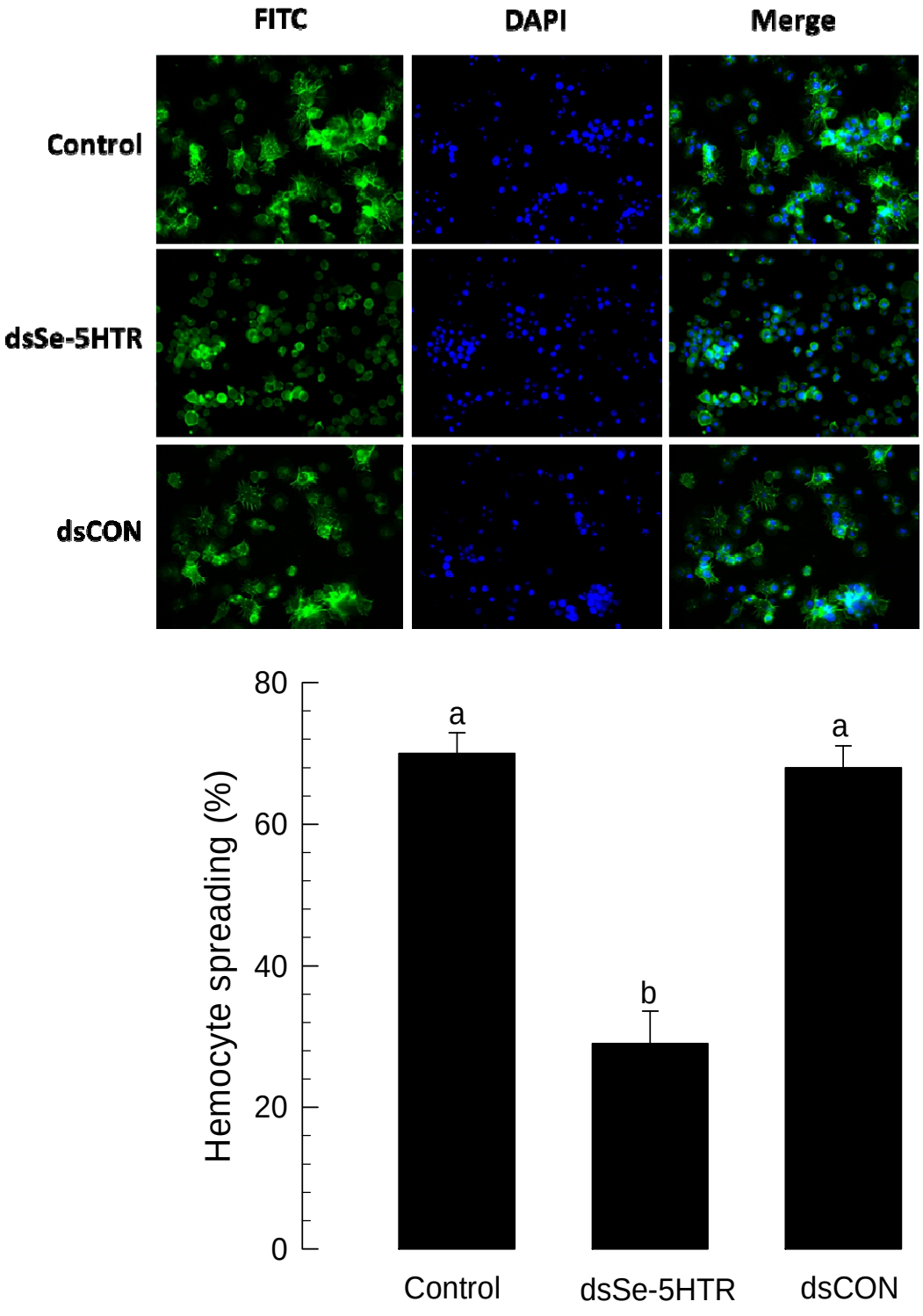

Fig. 4

bioRxiv preprint doi: https://doi.org/10.1101/556159; this version posted February 20, 2019. The copyright holder for this preprint (which was not certified by peer review) is the author/funder, who has granted bioRxiv a license to display the preprint in perpetuity. It is made available under aCC-BY 4.0 International license.

(A)

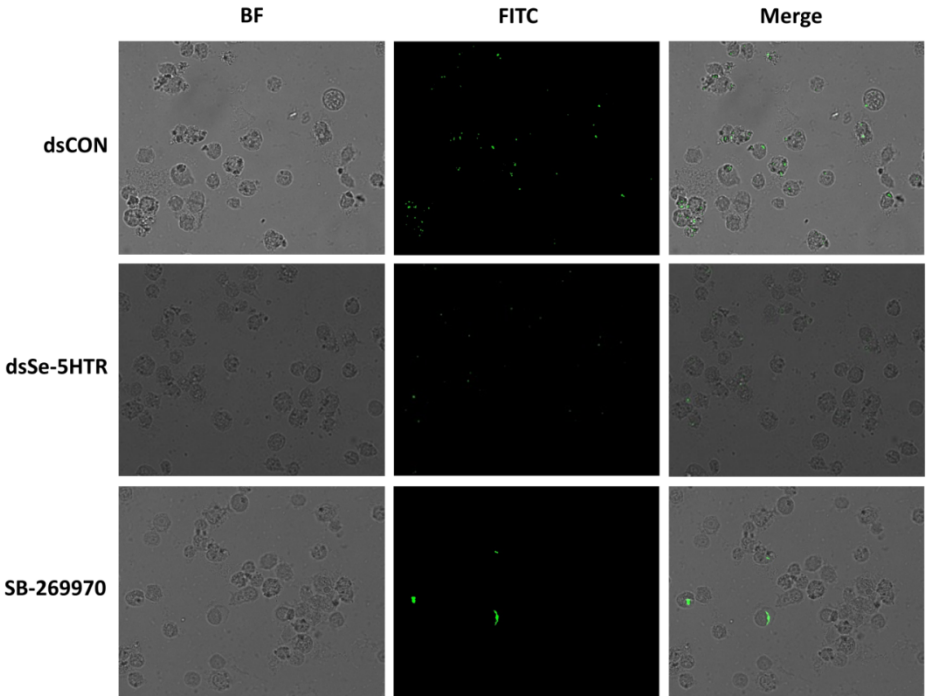

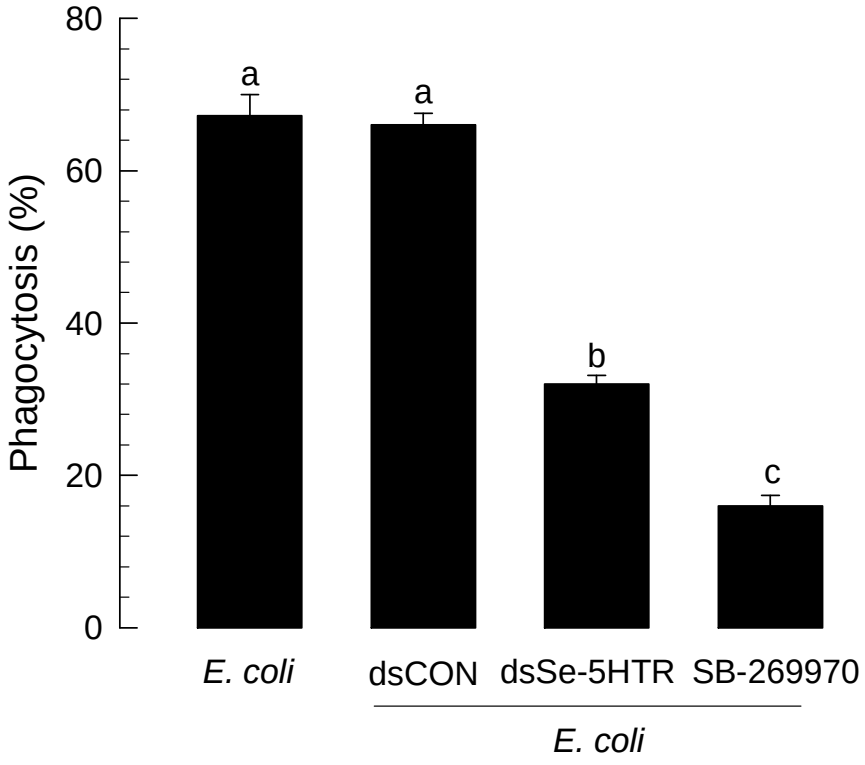

bioRxiv preprint doi: https://doi.org/10.1101/556159; this version posted February 20, 2019. The copyright holder for this preprint (which was not certified by peer review) is the author/funder, who has granted bioRxiv a license to display the preprint in perpetuity. It is made available under aCC-BY 4.0 International license.

(B)

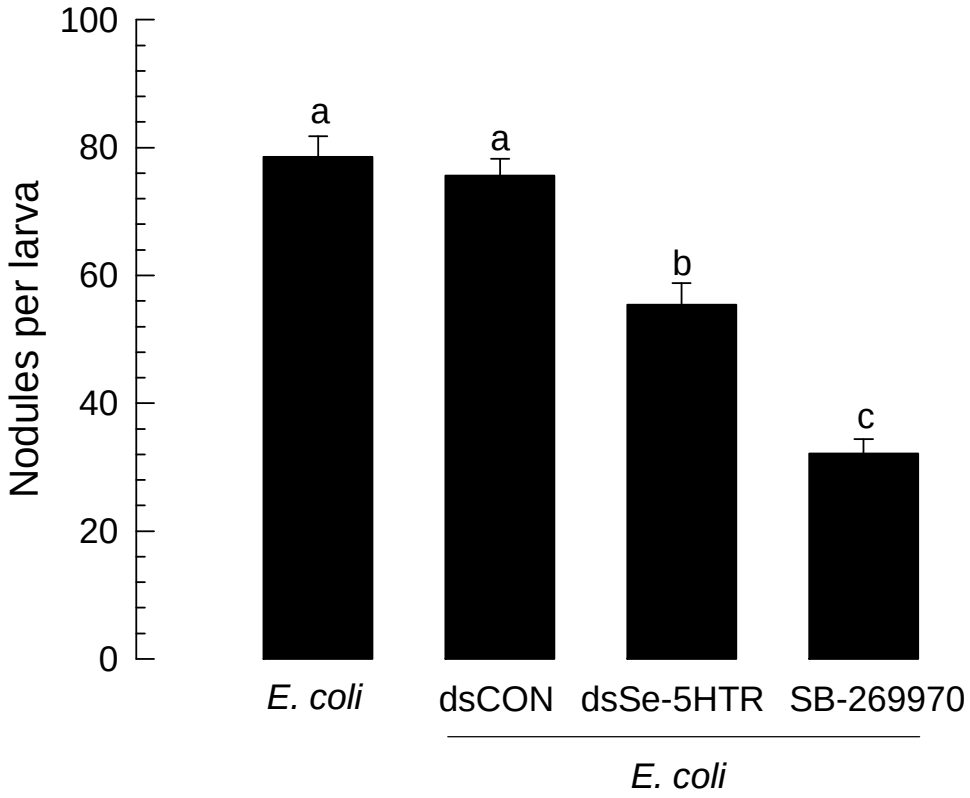

Fig. 5

bioRxiv preprint doi: https://doi.org/10.1101/556159; this version posted February 20, 2019. The copyright holder for this preprint (which was not certified by peer review) is the author/funder, who has granted bioRxiv a license to display the preprint in perpetuity. It is made available under aCC-BY 4.0 International license.

(A)

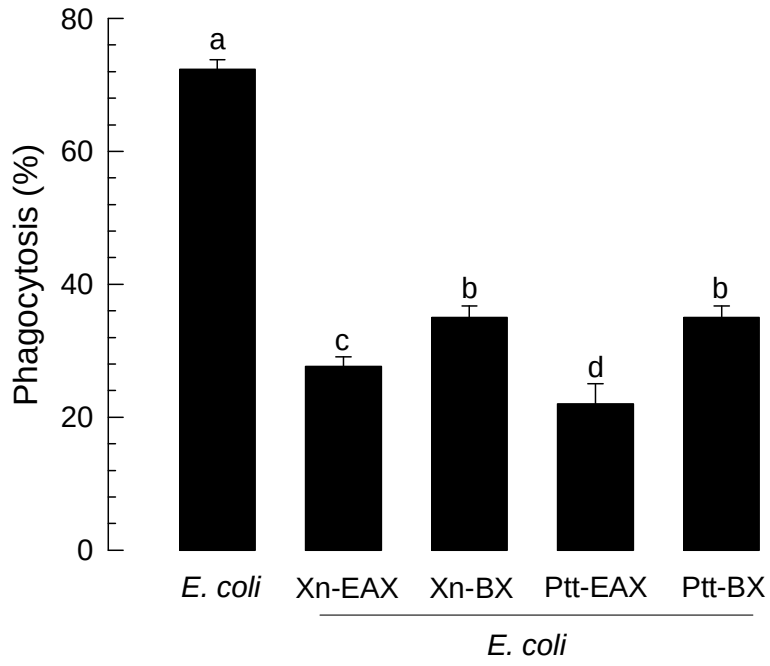

(B)

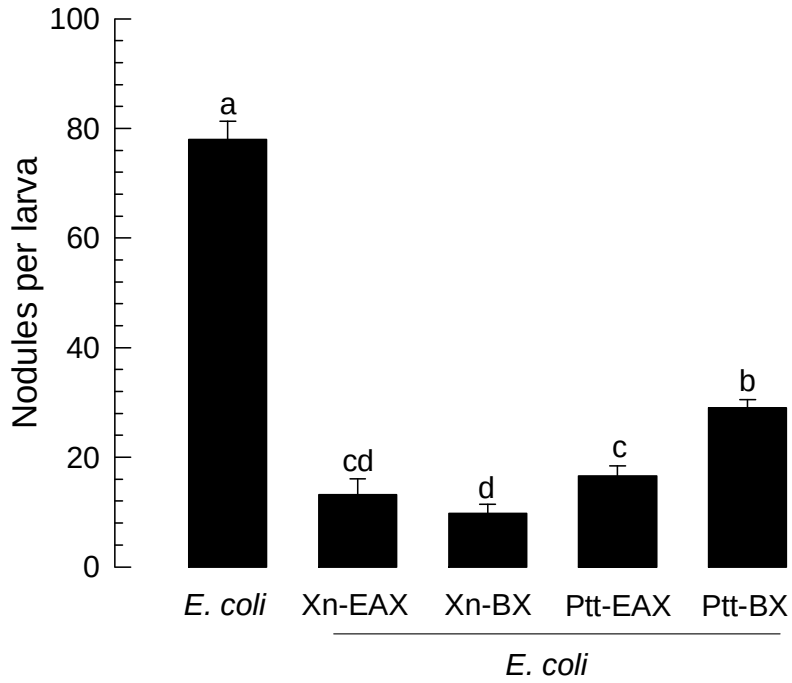

Fig. 6

bioRxiv preprint doi: https://doi.org/10.1101/556159; this version posted February 20, 2019. The copyright holder for this preprint (which was not certified by peer review) is the author/funder, who has granted bioRxiv a license to display the preprint in perpetuity. It is made available under aCC-BY 4.0 International license.

(A)

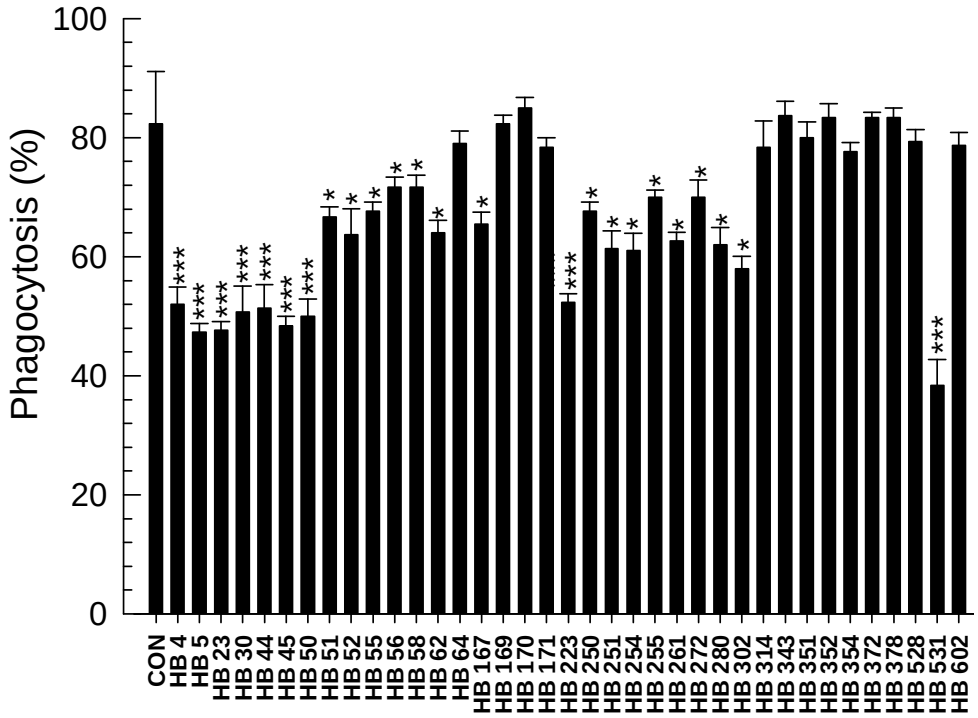

(B)

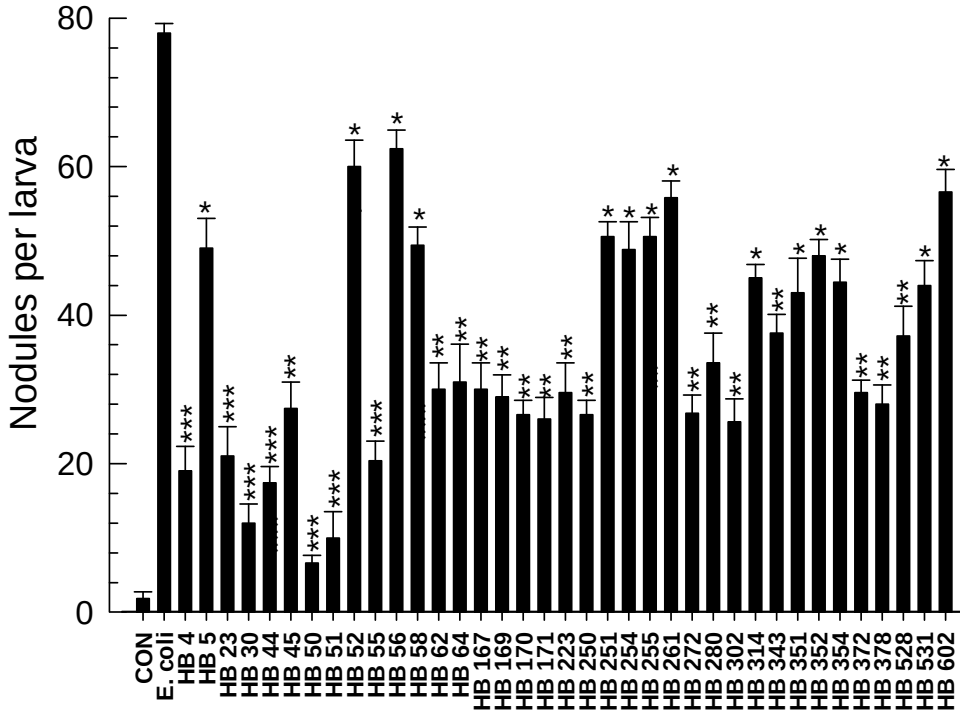

Fig. 7

bioRxiv preprint doi: https://doi.org/10.1101/556159; this version posted February 20, 2019. The copyright holder for this preprint (which was not certified by peer review) is the author/funder, who has granted bioRxiv a license to display the preprint in perpetuity. It is made available under aCC-BY 4.0 International license.

(A)

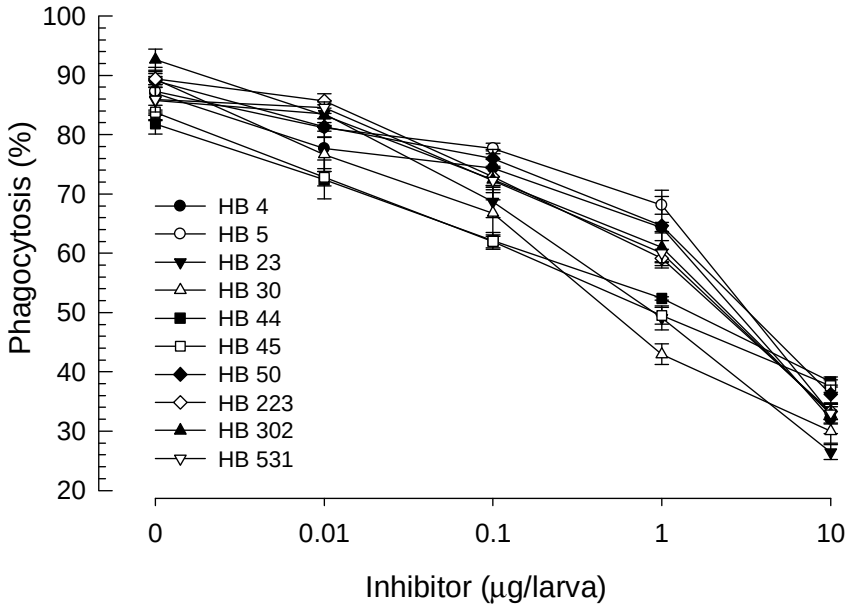

(B)

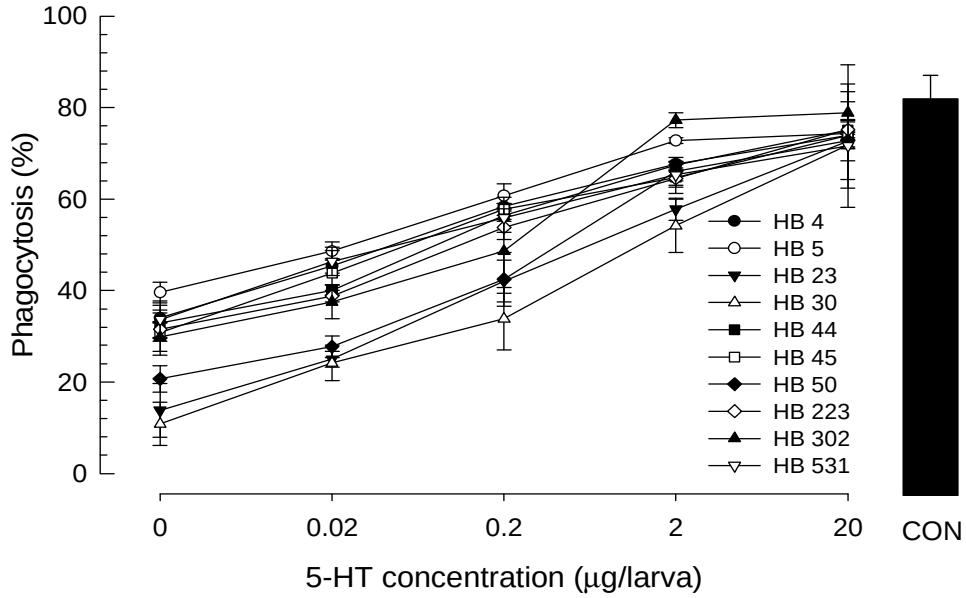

Fig. 8

bioRxiv preprint doi: https://doi.org/10.1101/556159; this version posted February 20, 2019. The copyright holder for this preprint (which was not certified by peer review) is the author/funder, who has granted bioRxiv a license to display the preprint in perpetuity. It is made available under aCC-BY 4.0 International license.

(A)

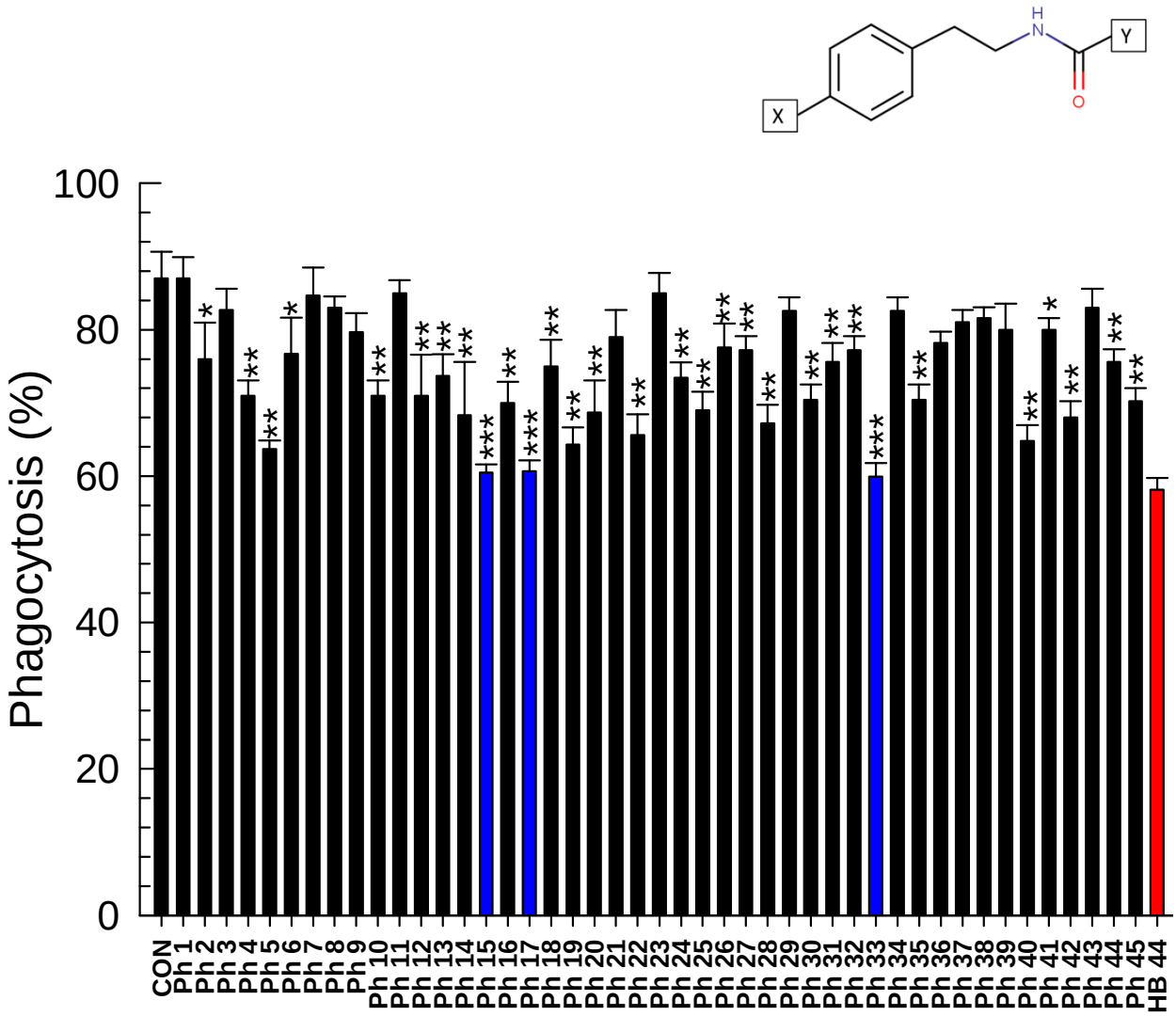

(B)

Compound	Structure	IC_{50} (μM)
Ph 15	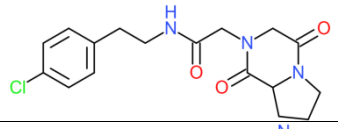	1.862 ± 0.221[c]
Ph 17	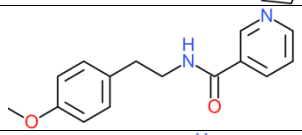	2.746 ± 0.078[b]
Ph 33	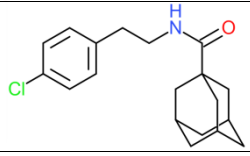	5.587 ± 0.98[a]

bioRxiv preprint doi: https://doi.org/10.1101/556159; this version posted February 20, 2019. The copyright holder for this preprint (which was not certified by peer review) is the author/funder, who has granted bioRxiv a license to display the preprint in perpetuity. It is made available under aCC-BY 4.0 International license.

(C)

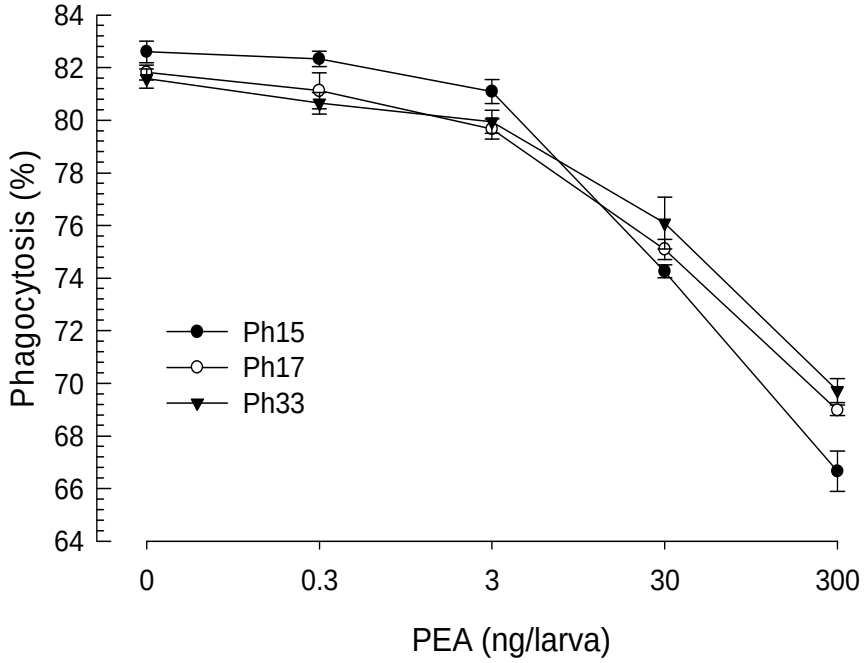

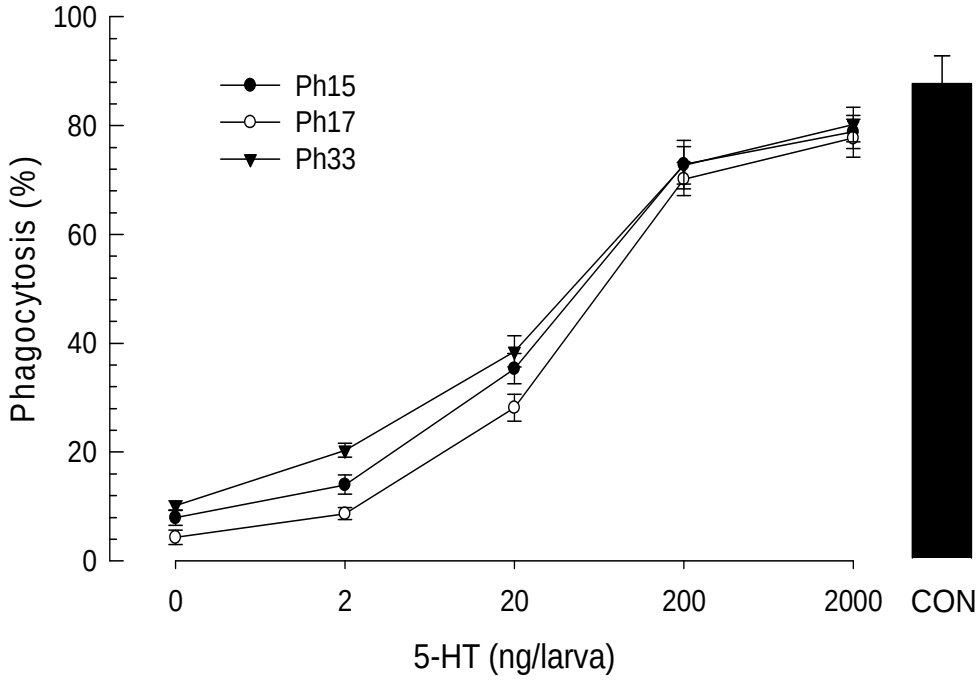

Fig. 9

bioRxiv preprint doi: https://doi.org/10.1101/556159; this version posted February 20, 2019. The copyright holder for this preprint (which was not certified by peer review) is the author/funder, who has granted bioRxiv a license to display the preprint in perpetuity. It is made available under aCC-BY 4.0 International license.

(A)

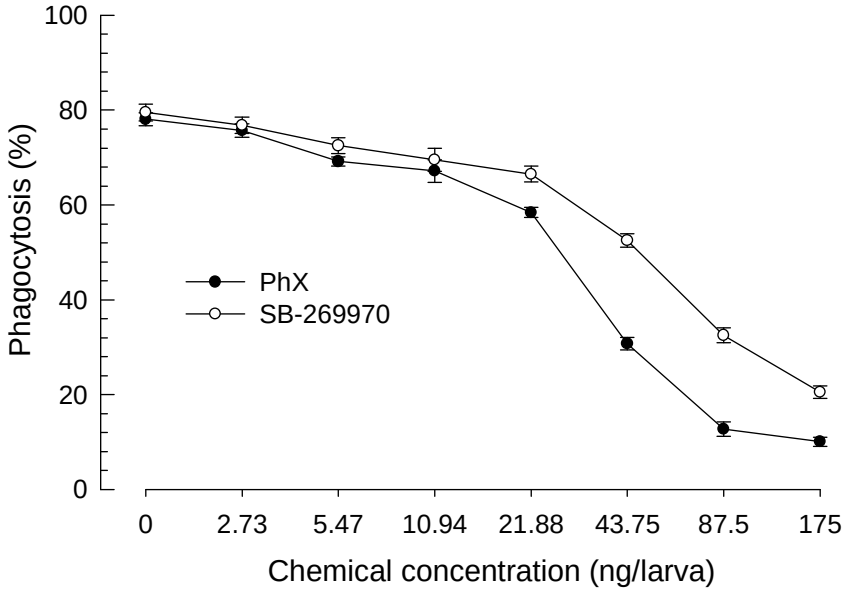

(B)

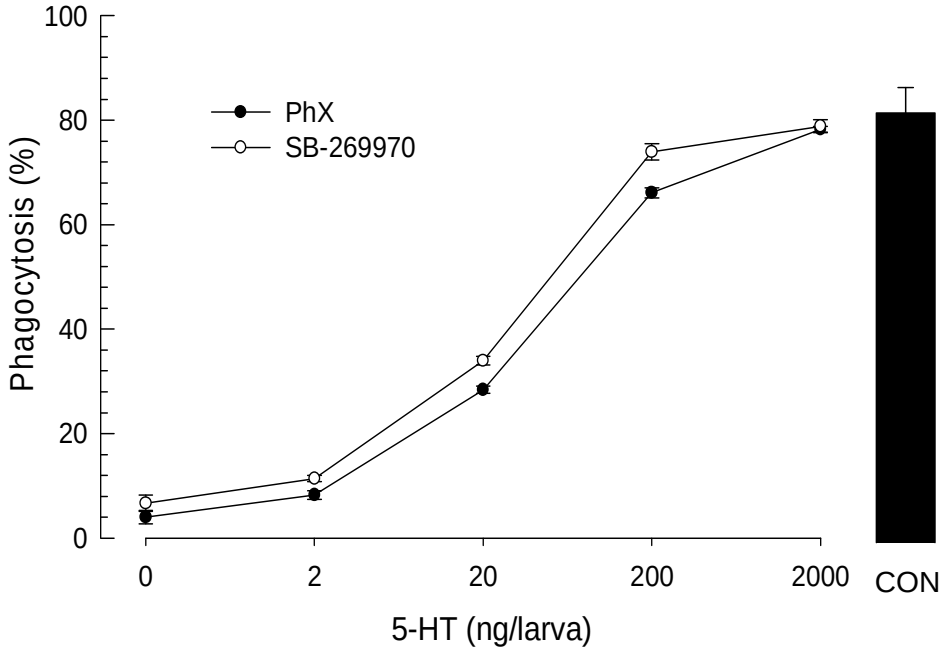

Fig. 10

bioRxiv preprint doi: https://doi.org/10.1101/556159; this version posted February 20, 2019. The copyright holder for this preprint (which was not certified by peer review) is the author/funder, who has granted bioRxiv a license to display the preprint in perpetuity. It is made available under aCC-BY 4.0 International license.

Supplementary data

S1 Fig. Putative domain and motif structures of Se-5HTR. Putative seven transmembrane domains (TM1-TM7) are primarily marked by dark yellow bars and circles. Extracellular and cytosolic regions are denoted by green and light blue regions, respectively. Potential N-glycosylation sites and phosphorylation sites are marked by orange and red circles, respectively. Aspartic acid residue (dark blue circle) in TM3 and serine residue (light brown circle) in TM5 are putative residues that might chemically interact with 5-HT. The unique consensus sequence motif (PXXXWXPXF, dark brown circles) in aminergic receptors is conserved in TM6. The motif (NPXXY, dark blue circles) is conserved in TM7 like other GPCRs. Two possible post-translational palmitoylation cysteine residues (light yellow circles) and a PDZ-domain binding motif (ESFL, black circles) are also present in the C-terminal. Conserved motifs were determined using InterPro tool (https://www.ebi.ac.uk/interpro/) and Prosite (http://prosite.expasy.org/) whereas other residues and motifs were predicted using several tools from DTU bioinformatics.

S2 Fig. Potent screened chemicals from HB compounds with their chemical structures and respective median inhibitory concentrations (IC_{50}). HB chemicals were injected in different doses (0, 0.01, 0.1, 1, and 10 µg/larva) along with a fixed 5-HT concentration (1 µg/larva) and FITC-tagged bacteria (500 cells/larva). After 15 min of treatment, hemocytes from treated larvae were collected in ACB followed by phagocytosis assay as described above. Percentages of phagocytosis against HB chemical treatment with increasing concentrations were calculated. Their IC_{50} values were determined using Probit analysis (https://probitanalysis.wordpress.com).

bioRxiv preprint doi: https://doi.org/10.1101/556159; this version posted February 20, 2019. The copyright holder for this preprint (which was not certified by peer review) is the author/funder, who has granted bioRxiv a license to display the preprint in perpetuity. It is made available under aCC-BY 4.0 International license.

S3 Fig. Designing a potent chemical inhibitor from phenylehtylamide (PEA) derivatives. Derivatives of PEA were tested for their nodulation inhibition percentages and sorted by their X and Y groups. Most potent residues inhibiting nodulation were selected and a hypothetical most potent PEA chemical was designed. (A) Core PEA structure with two variable hypothetical residues (X and Y). X belongs to the residue group attached with para position of the phenyl ring whereas Y belongs to the residue group linked to the amide group. (B) Comparative analysis between X residue groups with their mean percent inhibition of nodulation. (C) Comparative analysis between Y residue groups with their percent inhibition of nodulation. (D) A hypothetical PEA chemical compound structure having the most potent inhibition capability.

S4 Fig. Bacterial secondary metabolites (37 chemicals) derived from *Xenorhabdus* and *Photorhabdus*

S5 Fig. Phenylethylamide (PEA) derivatives (45 chemicals) based on HB 44, a bacterial metabolite

S6 Fig. Chemical synthesis of PhX ((*S*)-2-(1,4-dioxohexahydropyrrolo[1,2-*a*]pyrazin-2(*1H*)-yl)-*N*-(4-methoxyphenethyl)acetamide)

bioRxiv preprint doi: https://doi.org/10.1101/556159; this version posted February 20, 2019. The copyright holder for this preprint (which was not certified by peer review) is the author/funder, who has granted bioRxiv a license to display the preprint in perpetuity. It is made available under aCC-BY 4.0 International license.

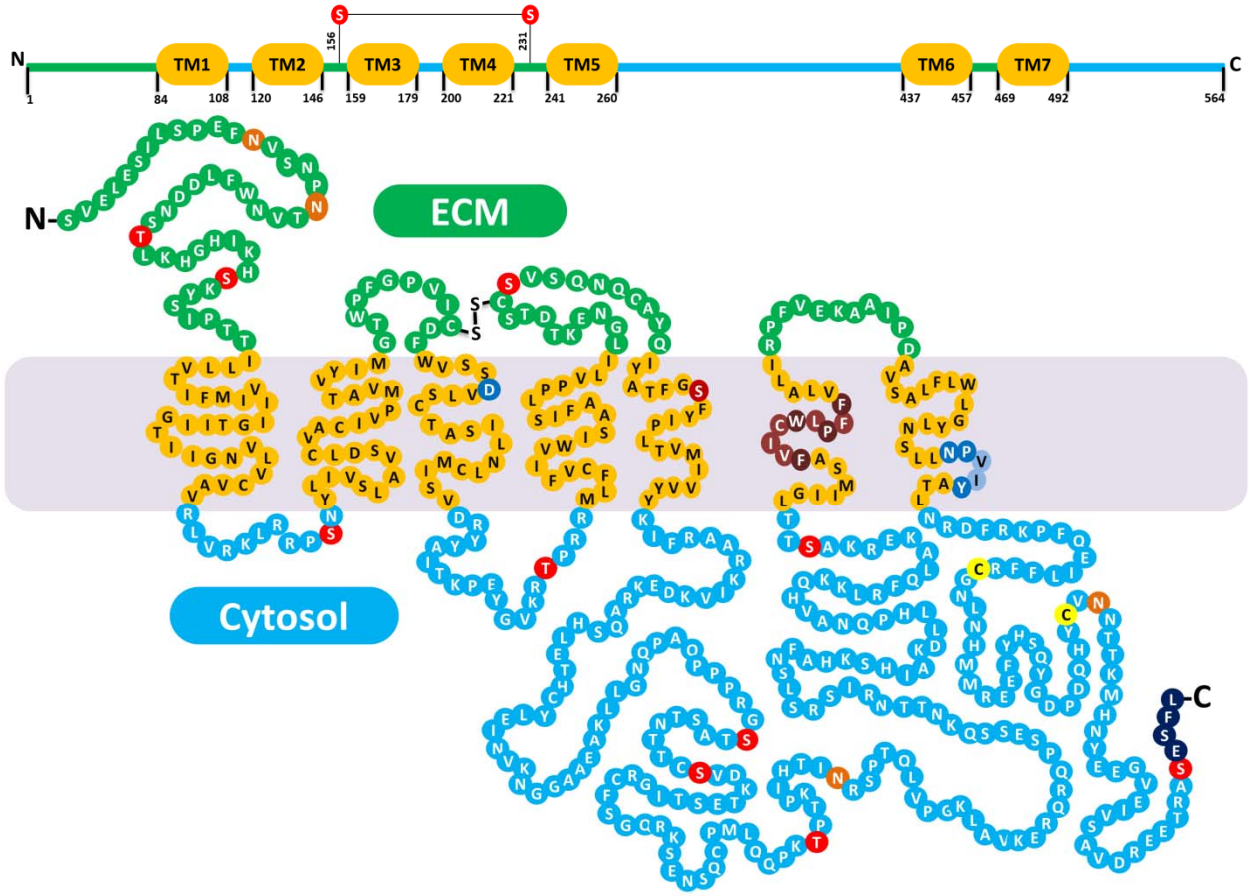

S1 Fig

bioRxiv preprint doi: https://doi.org/10.1101/556159; this version posted February 20, 2019. The copyright holder for this preprint (which was not certified by peer review) is the author/funder, who has granted bioRxiv a license to display the preprint in perpetuity. It is made available under aCC-BY 4.0 International license.

Groups	ID	Structure	IC_{50} (μM)
Phenylethylamide	HB 4	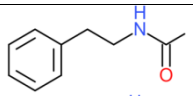	253.2 ± 38.0
	HB 5	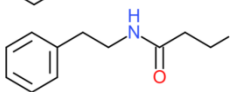	217.8 ± 43.6
	HB 44	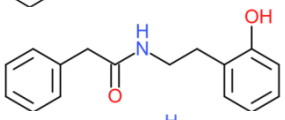	103.7 ± 18.7
Tryptamide	HB 23	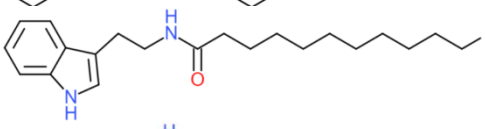	103.9 ± 15.6
	HB 50	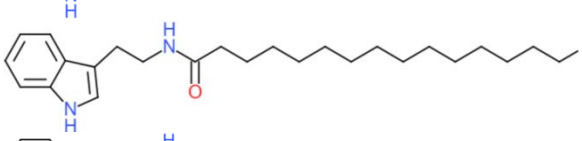	90.6 ± 16.3
	HB 531	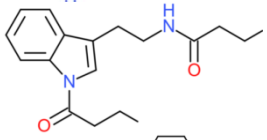	124.9 ± 23.7
Xenortide	HB 30	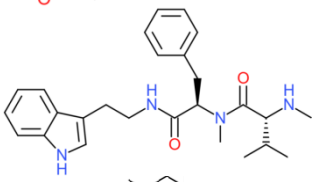	59.1 ± 9.5
Xenocyloin	HB 45	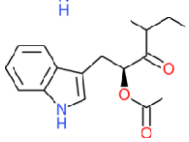	82.1 ± 14.8
Nematophin	HB 223	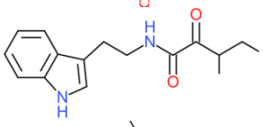	134. 6 ± 22.9
GameXPeptide	HB 302	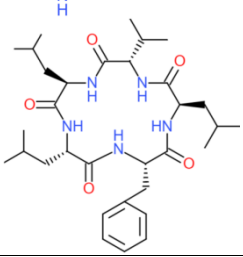	58.4 ± 11.7

S2 Fig

bioRxiv preprint doi: https://doi.org/10.1101/556159; this version posted February 20, 2019. The copyright holder for this preprint (which was not certified by peer review) is the author/funder, who has granted bioRxiv a license to display the preprint in perpetuity. It is made available under aCC-BY 4.0 International license.

(A)

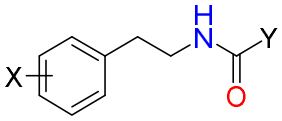

(B)

X	N	Inhibition of nodulation
4-OCH_3	2	80.9%
3,4-di-OCH_3	1	53.4%
4-Cl	3	49.6%
4-F	1	72.1%
4-CF_3	1	66.9%
4-H	2	62.7%

(C)

Y	Inhibition of nodulation
(X=4-Cl)	
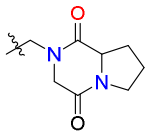	84.1%
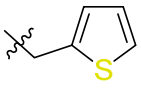	36.3%
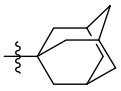	35.1%
(X=3,4-di-OMe)	
	77.7%
	77.3%
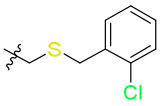	53.4%
(X=4-F)	
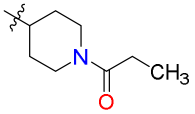	72.1%
(X=4-CF_3)	
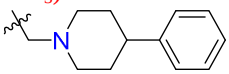	66.9%
(X=4-H)	
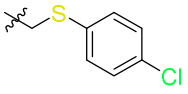	64.1%
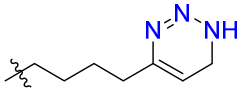	61.4%

(D)

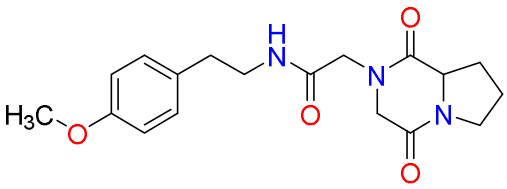

S3 Fig

bioRxiv preprint doi: https://doi.org/10.1101/556159; this version posted February 20, 2019. The copyright holder for this preprint (which was not certified by peer review) is the author/funder, who has granted bioRxiv a license to display the preprint in perpetuity. It is made available under aCC-BY 4.0 International license.

HB compound	Structure
HB 4	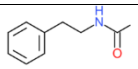
HB 5	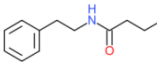
HB 23	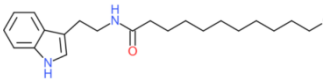
HB 30	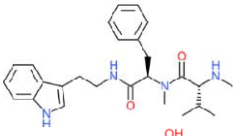
HB 44	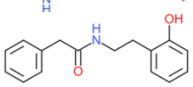
HB 45	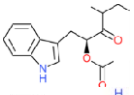
HB 50	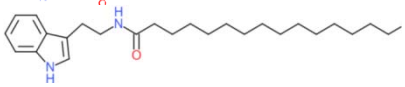
HB 51	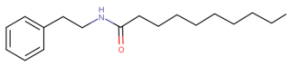
HB 52	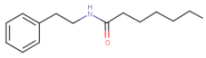
HB 55	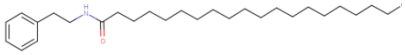
HB 56	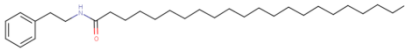
HB 58	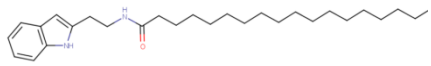

HB compound	Structure
HB 250	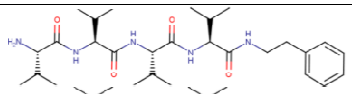
HB 251	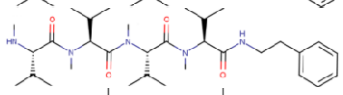
HB 254	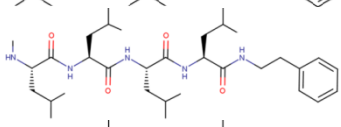
HB 255	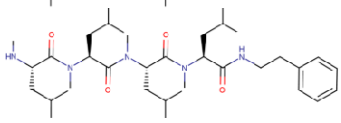
HB 261	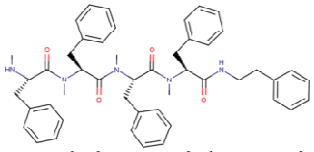
HB 272	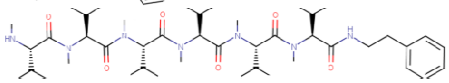
HB 280	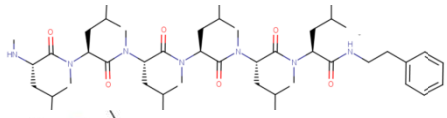
HB 302	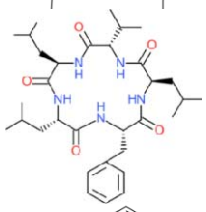
HB 314	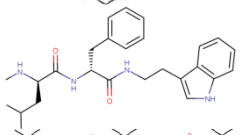
HB 343	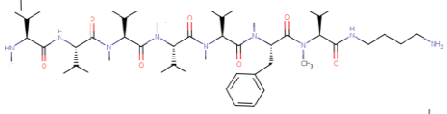
HB 351	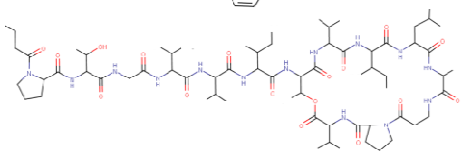
HB 352	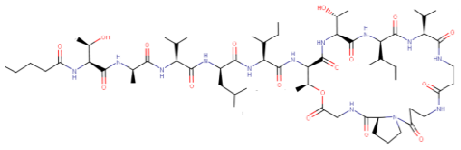

bioRxiv preprint doi: https://doi.org/10.1101/556159; this version posted February 20, 2019. The copyright holder for this preprint (which was not certified by peer review) is the author/funder, who has granted bioRxiv a license to display the preprint in perpetuity. It is made available under aCC-BY 4.0 International license.

HB 62

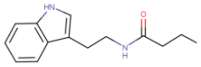

HB 64

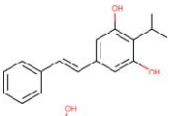

HB 167

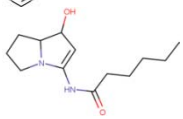

HB 169

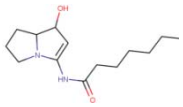

HB 170

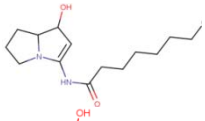

HB 171

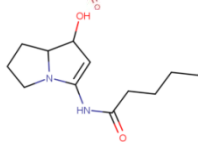

HB 223

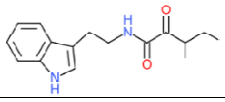

HB 354

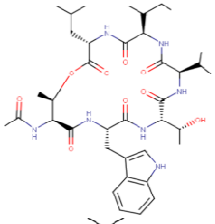

HB 372

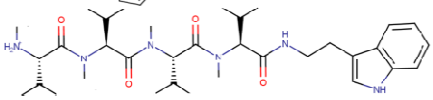

HB 378

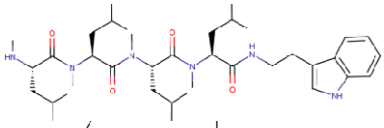

HB 528

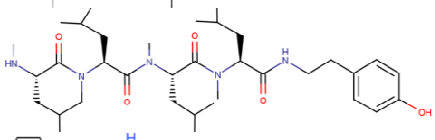

HB 531

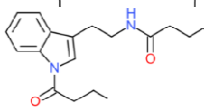

HB 602

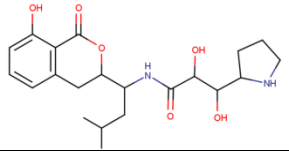

S4 Fig

bioRxiv preprint doi: https://doi.org/10.1101/556159; this version posted February 20, 2019. The copyright holder for this preprint (which was not certified by peer review) is the author/funder, who has granted bioRxiv a license to display the preprint in perpetuity. It is made available under aCC-BY 4.0 International license.

PEA compound	Structure
Ph 1	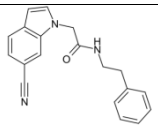
Ph 2	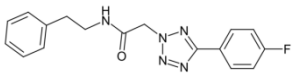
Ph 3	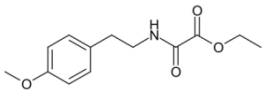
Ph 4	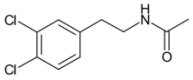
Ph 5	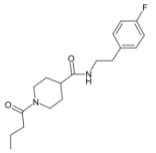
Ph 6	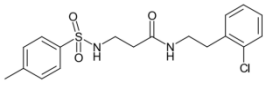
Ph 7	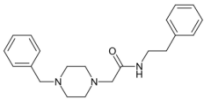
Ph 8	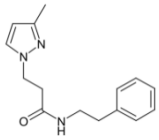
Ph 9	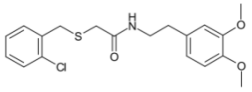
Ph 10	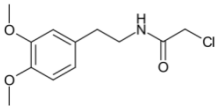
Ph 11	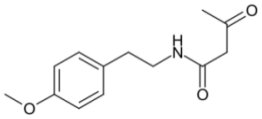
Ph 12	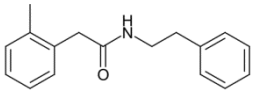

PEA compound	Structure
Ph 24	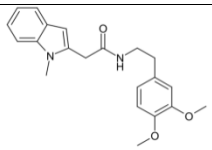
Ph 25	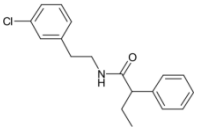
Ph 26	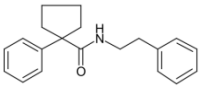
Ph 27	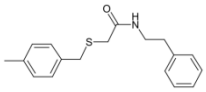
Ph 28	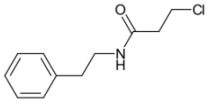
Ph 29	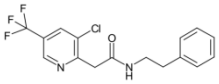
Ph 30	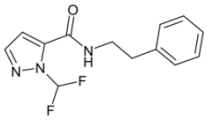
Ph 31	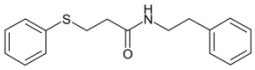
Ph 32	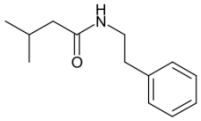
Ph 33	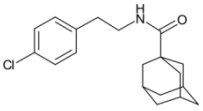
Ph 34	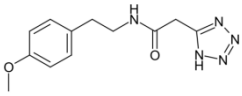
Ph 35	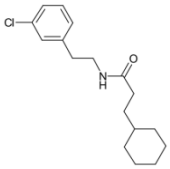

bioRxiv preprint doi: https://doi.org/10.1101/556159; this version posted February 20, 2019. The copyright holder for this preprint (which was not certified by peer review) is the author/funder, who has granted bioRxiv a license to display the preprint in perpetuity. It is made available under aCC-BY 4.0 International license.

Ph 13 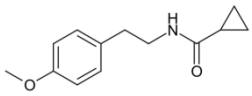

Ph 14 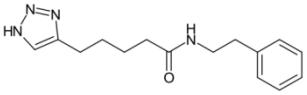

Ph 15 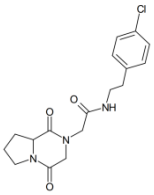

Ph 16 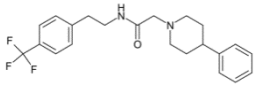

Ph 17 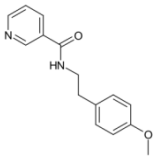

Ph 18 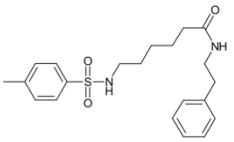

Ph 19 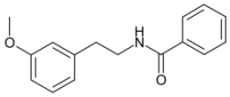

Ph 20 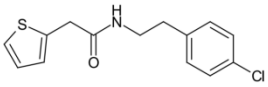

Ph 21 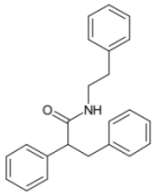

Ph 22 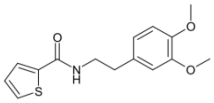

Ph 23 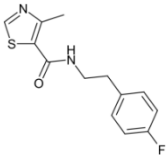

Ph 36 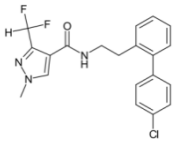

Ph 37 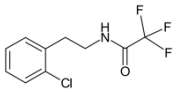

Ph 38 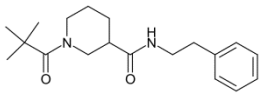

Ph 39 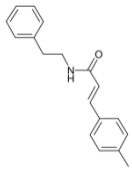

Ph 40 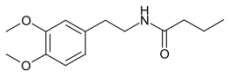

Ph 41 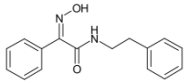

Ph 42 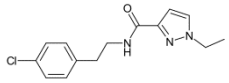

Ph 43 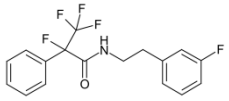

Ph 44 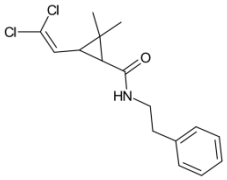

Ph 45 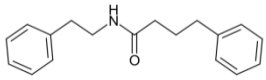

S5 Fig

bioRxiv preprint doi: https://doi.org/10.1101/556159; this version posted February 20, 2019. The copyright holder for this preprint (which was not certified by peer review) is the author/funder, who has granted bioRxiv a license to display the preprint in perpetuity. It is made available under aCC-BY 4.0 International license.

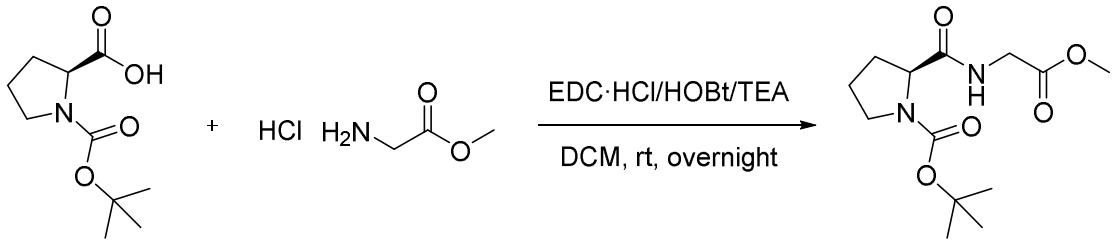

1 **2** **3**

Step 1

Synthesis of (*S*)-(-)-*N*-(*t*-butoxycarbonyl)-prolylglycine methylester (**3**)

To a solution of (S)-(-)-N-(t-butoxycarbonyl)-proline **1** (5.00 g, 23.0 mmol) in CH_2Cl_2 (150 mL), amino acid methyl ester hydrochloride **2** (2.89 g, 23.0 mmol), 1-[3-(dimethylamino)propyl)]-3-ethylcarbodiimide hydrochloride (5.34 g, 28.0 mmol), and 1-hydroxybenzotriazole monohydrate (3.77 g, 28.0 mmol) triethylamine (6.50 mL, 46.6 mmol) were added and the reaction mixture was stirred for 24 h at room temperature. The solvent was removed under reduced pressure. The residue was taken up in ethyl acetate (200 mL) and washed successively with water (200 mL), 1N HCl aqueous solution (200 mL), and sat. $NaHCO_3$ aqueous solution (200 mL). The solvent was removed under reduced pressure to give (*S*)-(-)-*N*-(*t*-butoxycarbonyl)-prolylglycine methylester **3** as a white solid (4.82 g, 73%).

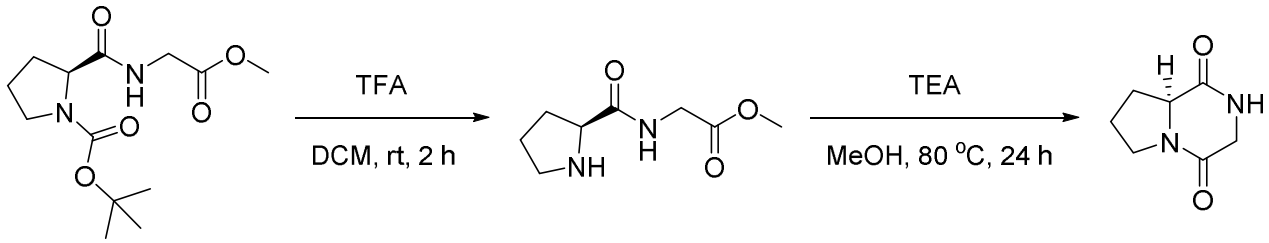

3 **4** **5**

Step 2

Synthesis of (*S*)-Hexahydropyrrolo[1,2-*a*]pyrazine-1,4-dione (**5**)

To a solution of (*S*)-(-)-*N*-(*t*-Butoxycarbonyl)-prolylglycine methylester **3** (4.80 g, 16.8 mmol) in CH_2Cl_2 (84 mL), trifluoroacetic acid (18.7 mL, 252.0 mmol) was added and the solution was stirred at room temp for 2 hr. The solvent was removed under reduced pressure. The residue was dissolved in MeOH (84 mL) and treated with triethylamine (9.3 mL, 67.2 mmol). The reaction mixture was kept under reflux overnight. The solvent was removed under reduced pressure and the oily residue was redissolved in *i*-propanol to give (*S*)-hexahydropyrrolo[1,2-*a*]pyrazine-1,4-dione **5** as a white solid (2.0 g, 78%).

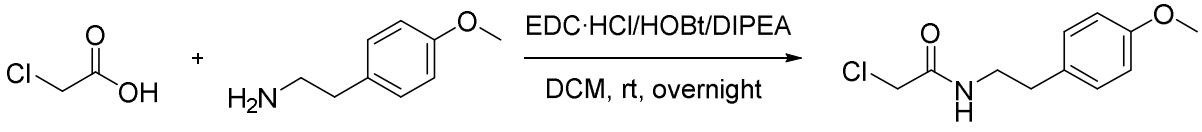

6 **7** **8**

bioRxiv preprint doi: https://doi.org/10.1101/556159; this version posted February 20, 2019. The copyright holder for this preprint (which was not certified by peer review) is the author/funder, who has granted bioRxiv a license to display the preprint in perpetuity. It is made available under aCC-BY 4.0 International license.

bioRxiv preprint doi: https://doi.org/10.1101/556159; this version posted February 20, 2019. The copyright holder for this preprint (which was not certified by peer review) is the author/funder, who has granted bioRxiv a license to display the preprint in perpetuity. It is made available under aCC-BY 4.0 International license.

Step 3

Synthesis of 2-chloro-*N*-(4-methoxyphenethyl)acetamide (**7**)

To a solution of 2-chloroacetic acid **6** (3.00 g, 31.8 mmol) in CH_2Cl_2 (160 mL), 2-(4-methoxyphenyl)ethylamine **7** (4.6 mL, 31.8 mmol) and *N*,*N*-diisopropylethylamine (8.45 mL, 63.5 mmol) were added and the reaction mixture was stirred for 15 min at room temperature. After addition of 1-[3-(dimethylamino)propyl)]-3-ethylcarbodiimide hydrochloride (7.30 g, 38.1 mmol) and 1-hydroxybenzotriazole monohydrate (5.14 g, 38.1 mmol), the reaction mixture was stirred for 24 h at room temp. The reaction mixture was washed successively with 1 N HCl aqueous solution (160 mL) and sat. $NaHCO_3$ aqueous solution (160 mL). The organic layer was dried over $MgSO_4$, filtered, and concentrated. The residue was washed with diethyl ether to give 2-chloro-*N*-(4-methoxyphenethyl)acetamide **8** as a yellow solid (4.60 g, 63%).

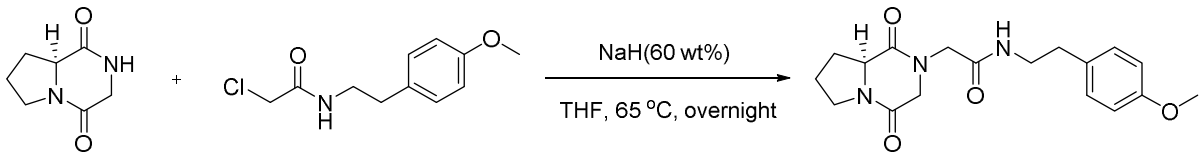

5 **8** **9**

Step 4

Synthesis of (*S*)-2-(1,4-dioxohexahydropyrrolo[1,2-*a*]pyrazin-2(*1H*)-yl)-*N*-(4-methoxyphenethyl)acetamide (**9**)

To a solution of (*S*)-hexahydropyrrolo[1,2-*a*]pyrazine-1,4-dione **5** (1.00 g, 6.40 mmol) in THF (32 mL), portionwise 60 wt% NaH (260 mg, 6.40 mmol) at 0°C was added and the reaction mixture was stirred 15 min at room temperature. 2-chloro-*N*-(4-methoxyphenethyl)acetamide **7** was added slowly to the reaction mixture then the mixture was stirred overnight at 65°C. The reaction was monitored by TLC. The reaction mixture was quenched with sat. NH_4Cl aqueous solution (100 mL) and extracted with EtOAc (2 X 100 mL). Combined organic layers were dried over MgSO4, filtered, and concentrated. The crude product was purified by silica-gel column chromatography (eluent: MeOH 10% in CH_2Cl_2) to give (*S*)-2-(1,4-dioxohexahydropyrrolo[1,2-*a*]pyrazin-2(*1H*)-yl)-*N*-(4-methoxyphenethyl)acetamide **9** as a yellow foam (1.74 g, 79%).

S6 Fig